TR-156
1993

Effectiveness of Native Species Buffer Zones for Nonstructural Treatment of Urban Runoff

R.H. Glick
M.L. Wolfe
T.L. Thurow

Texas Water Resources Institute

Texas A&M University

TR-156

Effectiveness of Native Species Buffer Zones for Nonstructural Treatment of Urban Runoff

Roger H. Glick

Mary Leigh Wolfe

Thomas L. Thurow

Texas Water Resources Institute

Texas A&M University

October 1993

RESEARCH COMPLETION REPORT

EFFECTIVNESS OF NATIVE SPECIES BUFFER ZONES FOR NONSTRUCTURAL TREATMENT OF URBAN RUNOFF

Project Number - 03

(September 1, 1989 - August 31, 1992)

Grant Number

14-08-0001-G2048

by

Roger H. Glick
USDA Fellow
Agricultural Engineering
Texas A&M University
College Station TX

Mary Leigh Wolfe
Associate Professor
Agricultural Engineering
Virginia Polytechnic Institute
& State University
Blacksburg VA

Thomas L. Thurow
Associate Professor
Rangeland Ecology
& Management
Texas A&M University
College Station TX

The research on which this report is based was financed in part by the Department of the Interior, U.S. Geological Survey, through the Texas Water Resources Institute. Non-Federal matching funds were provided by the City of Austin, Texas.

Technical Report No. 156
Texas Water Resources Institute
The Texas A&M University System
College Station, Texas 77843-2118

October 1993

Effectiveness of Native Species Buffer Zones for Nonstructural Treatment of Urban Runoff

Abstract

A field study was conducted to determine the influences of vegetation composition, buffer width, and infiltration rate on the effectiveness of native vegetation buffer zones as nonstructural treatments of urban runoff with respect to increasing water quality. The field site was in Austin, Texas with runoff originating in a parking lot with a drainage area of approximately one hectare. The soil was a shallow, well-drained clay overlying limestone. Twelve constituents were measured; fecal streptococci, fecal coliforms, dissolved nitrate, total nitrate, dissolved total phosphorus, total phosphorus, dissolved ammonia, total ammonia, dissolved total Kjeldahl nitrogen, total Kjeldahl nitrogen, total lead, and total suspended solids. Four different vegetation compositions were used as treatments; wooded areas, wooded areas cleared, native grasses mowed, and native grasses unmowed. The vegetation in the mowed and unmowed areas was primarily composed of Johnson grass (*Sorghum halepense*), Bermuda grass (*Cynodon dactylon*) and mixed legumes. The wooded area was dominated by common red cedar (*Juniperus virginiana*) with scattered live oak (*Quercus virginiana*) and Ashe juniper (*Juniperus ashei*). The ground cover was juniper litter and scattered Texas wintergrass (*Stipa leucotricha*).

Only total suspended solids, total lead, total Kjeldahl nitrogen, total nitrate, total phosphorus, dissolved nitrate, and dissolved total phosphorus were influenced at the 0.10 significance level by vegetation composition and buffer width. For pollutants affected by vegetation composition, the wooded areas had the highest mean concentrations of pollutants. The mowed and unmowed areas generally had the lowest concentrations of pollutants. For this application of buffer strips, it was found that as buffer width increased, the pollutant concentration also increased. Other researchers have reported decreasing pollutant concentrations. One explanation is that this is caused by excess transport capacity associated with

the runoff entering the buffer strip. As the runoff moved though the buffer strip, pollutants were detached and transported through the buffer strip. If the buffer strip is sufficiently wide, an equilibrium between detachment and transport capacity may be reached and a decrease in pollutant concentration may be seen subsequently.

A physically-based model was developed to simulate sediment yield through the buffer strips studied. The model has a stochastic pollutant concentration input generator. Transport capacity is computed using the Yalin equation. Detachment and deposition are computed using a modified version of the Universal Soil Loss Equation. The model was used to simulate this field study. The model did not simulate individual rainfall events well. The model predicted the long-term average results of this field study with concentrations increasing with buffer width. The coefficient of determination for observed concentrations compared to average predicted concentrations was 0.90.

Contents

List of Figures

List of Tables

1 Introduction

Nonpoint source pollution is a major contributor to decreasing water quality in lakes, streams, and rivers. Nonpoint source pollution comes from a diffuse source such as a field or parking lot, as opposed to a point discharge like a sewer pipe or industrial discharge. Many land uses and management practices are contributors to nonpoint source pollution. Construction sites and surface mines have been identified as sources of sediment and some agricultural practices are linked to the production of nonpoint source pollutants including sediment, nitrogen, phosphorus, and pesticides. More recently, nonpoint source pollution has been identified as a source of pollutants in urban watersheds. Pollutants of concern in urban areas include sediment, nitrogen, phosphorus, and pesticides, as well as oil, grease, lead, other metals, and toxic substances. The runoff from lawns, especially in suburban residential areas, is a possible source of pollution from lawn fertilizer, pesticides, and fecal coliforms (Kelling and Peterson, 1975). Runoff from roads and parking lots is a probable source of oil, grease, lead, and other toxic substances.

Urban runoff contributes to increased nonpoint source pollution, compared to undeveloped or natural areas, in several ways. The most important are (1) an increase in runoff volume compared to natural land patterns and (2) the increased erosive force associated with the increased runoff. The increase in runoff can be attributed to the increase in impervious areas, including roofs, roads, and parking lots. Even though the impervious portion of a catchment is small, it is responsible for the majority of runoff in most events (Bufill and Boyd, 1988). The increase in impervious areas is also responsible for increasing the peak and reducing the duration of the runoff event. This may require expensive flood control structures such as dams, detention ponds, and settling basins to control flooding and to help control nonpoint source pollution. When the runoff enters pervious or erodible areas, it produces more sediment and other debris because of the increased erosive forces and increased transport capacity associated with the increase in runoff rates. The increase in sediment loading in streams is a major source of water quality degradation.

The pervious areas in an urban watershed can also contribute to an increase in runoff. The infiltration rate for maintained lawns can be as low as one-sixth of that for land remaining in native vegetation. This reduction is very significant because 35 to 85% of the total surface area in an urban watershed may be maintained in lawns. The decrease in infiltration rate may be caused by compaction during construction, or by disturbance of the natural soil profile by adding or removing topsoil during landscaping (Kelling and Peterson, 1975). Research has indicated that vegetation type also affects infiltration and runoff rates (Dunne et al., 1988; Thurow et al., 1988).

Local and regional regulations are being proposed in many areas to limit the stream loading from urban stormwater runoff. The U.S. Environmental Protection Agency has begun the process of requiring large municipalities to acquire storm water discharge permits through the National Pollutant Discharge Elimination System (NPDES) program. A number of management practices have been proposed for reducing the delivery of pollutants to streams. Many municipalities require or recommend the use of detention ponds or settling basins to capture urban runoff (Parrish and Stecher, 1991). Outlet structures and stream channel improvements may be required to reduce the effects of the erosive forces. These structures and others like them are expensive and, in many cases, not aesthetically pleasing. The use of effective nonstructural runoff control practices is desired in many places.

One practice that has gained attention in recent years is the use of vegetated buffer strips located between the contributing area and the receiving stream or lake. Some cities, such as Austin TX, Baltimore MD, and Denver CO, have passed ordinances requiring the use of buffer zones in all developing areas to reduce the pollution potential from those areas. Some states, including North Carolina, Maryland, and Virginia, along with the U.S. Department of Agriculture are promoting the use of filter strips on agricultural lands. Design criteria and performance expectations are quite variable due to the lack of information available on processes which determine vegetative buffer strip effectiveness.

Buffer strips have benefits that extend beyond filtering pollutants. Streams with broad wooded buffers exhibit less of a tendency to erode (Whipple et al., 1983). Except in very flat

areas or areas with good buffer strips, urbanization will almost always result in an erosive disequilibrium. The imbalance in the stream is caused mainly by a decrease in runoff duration and an increased peak runoff during storm events. This disequilibrium is characterized by stream bed lowering and channel enlargement and deepening. This channel degradation is not self-corrective and will move upstream into smaller tributaries.

Vegetated buffer strips reduce pollutants in runoff by changing the flow characteristics of the runoff water. By slowing the velocity of the water, sediment and pollutants adsorbed to the sediment are deposited in the buffer strip. Secondly, the slower flow rate allows more opportunity time for the runoff to infiltrate into the soil in the buffer zone. In this manner, the amount of runoff with dissolved pollutants may be reduced. The processes through which buffer strips affect runoff quality are dependent on parameters such as slope, buffer width, soil type, and vegetation type. Design guidelines have not yet been developed for vegetated buffer strips. To date, strips have been designed based on professional judgment and trial and error because no acceptable design procedure has been set forth (Dillaha et al., 1989). With the increasing need for buffer strip design information, it is essential that scientifically-based design guidelines be developed as soon as possible.

The objectives of the research conducted for this project were:

1. To determine the influences of vegetation composition, slope, buffer width, and infiltration rate on the effectiveness of native vegetation buffer zones as nonstructural treatment of urban runoff with respect to increasing water quality. The following hypotheses were tested:

   (a) The vegetation composition of the buffer influences its effectiveness.

   (b) As the slope of a buffer strip increases, its effectiveness decreases.

   (c) As the width of a buffer strip increases, its effectiveness increases.

   (d) As the infiltration rate of the soil in a buffer increases, the buffer effectiveness increases.

2. To determine the relative importance of vegetation composition, slope, buffer width, and infiltration rate on the effectiveness of native vegetation buffer zones.

3. To evaluate, and refine where possible, existing mathematical buffer strip models for applicability in urban areas.

4. To perform sensitivity analyses of the buffer strip model that best simulates urban buffer strips to determine the variables influencing the model results and compare these to factors influencing buffer effectiveness determined by the field study.

2 Literature Review

Prior studies of buffer strips can be divided field research and model development. Field research related to vegetative buffer strips has focused mainly on land application of animal waste or protection of shorelines. Other studies have focused on reducing sediment in runoff from row cropping, mining, and forestry operations. The use of field and watershed scale hydrologic models to simulate buffer strips has been explored, but most of the modeling research has concentrated on developing models specifically for buffer strips.

2.1 Field Research

In one of the earlier studies, Wilson (1967) proposed buffer lengths of 3.05, 15.24, and 121.92 m (10, 50, and 400 ft) for the maximum removal of sand, silt, and clay, respectively, but presented no analytical results. Wilson did observe that submerged grass filters were less effective than filters that were not submerged.

Several studies have been conducted to determine the effectiveness of buffer strips in removing pollutants. Doyle et al. (1977) evaluated both a forested watershed as the buffer and a constructed grass buffer with manure as the pollution source. The forested area had deciduous trees with honeysuckle (*Honicero*) as the groundcover. Doyle et al. found that the greatest reduction of nutrients in the forested buffer was in the first 3.8 m. Total nitrogen was reduced by 94.7%, phosphorus by 99.5%, and potassium by 95.2% compared to incoming levels. Fecal coliforms and fecal streptococci were reduced 42 and 56%, respectively, in the first 3.8 m without a significant reduction thereafter. The constructed grass buffer strips were planted with Kentucky 31 tall fescue (*Festuca* sp.). The results were compared with a similar grass control plot that did not have a manure application. The loading rates for ammonia nitrogen, potassium, sodium, fecal coliforms, and fecal streptococci were reduced to levels near that of the control plot within 4 m. Loading rates for nitrate were reduced to near background levels with a 1.5 m buffer width. Phosphorus was reduced by 62% in the

4 m strip, but was still twice as high as the control.

Neibling and Alberts (1979) researched the length of bluegrass sod (*Poa pratensis*)buffer strip needed to remove different sediment particle sizes. The researchers found that with a buffer strip 1.22 m wide the sediment was reduced by 78%; after that the additional reduction was less than 5% to 4.88 m. They recommended that the buffer not be wider than 1.22 m if the goal is just mass reduction of sediment, but if smaller particles (less than 0.01 mm) are to be removed also, the buffer strip may need to be as wide as 2.44 m.

Bingham et al. (1980) conducted research using poultry litter as a pollutant, and checked concentrations of chemical oxygen demand, total Kjeldahl nitrogen, total phosphorus, chlorides, and total organic carbon. The buffer was originally seeded in reed canarygrass (*Calamagrostis* sp.), fescue (*Festuca* sp.), and redtop (*Agrostis* sp.). The results suggested that a buffer area length to waste area length ratio of one reduces the pollutant concentration to near that of the runoff not going through the waste area. The length ratio could be lower if pollutant concentrations greater than that of the background runoff were acceptable. It was noted that this data may not be valid if the waste area and buffer area are not similar in vegetative cover, surface soil condition or hydrologic properties.

Researchers in Virginia (Dillaha et al., 1989) found that buffers were more effective during initial rainfall events after buffer construction. This was attributed to sediment build-up in the buffer strip. The researchers found that sediment reduction ranged from 70 to 98% for a 9.1 m buffer. Total nitrogen and total phosphorus yields followed the same trend as sediment. Total nitrogen was reduced by 66% and phosphorus was reduced by 65 to 95%. Reduction in soluble phosphorus was variable ranging from 70 to -192%. No explanation was given for the increase in soluble phosphorus. The study was conducted on buffers with orchardgrass as the vegetation. reduction in runoff was also measured. On test plots with 11% slope, the runoff volume was reduced up to 74%. On test plots with cross slopes to simulate concentrated flow, runoff was reduced up to 72%. On test plots with 16% slope, runoff was not reduced.

A review of buffer strip research in forestry areas (Clinnick, 1985) concluded that a 30 m buffer will protect water quality in most cases. A 20 m buffer might give adequate protection if the soils are highly permeable and the stream side slope is less than 30%. If the slope is greater than 30%, a wider buffer will be required to protect the water quality of the stream. The reviewer also noted that a continuous narrow buffer starting at the source of the ephemeral drainage area is more likely to be effective than a single wide buffer at the pollution source. No new research was done to support the conclusions and no data were presented.

Lowrance et al. (1984) studied the nutrient uptake of riparian forest used as agricultural buffers. They found that the hardwood forest acted as a sink for the nutrients entering the system. Nitrogen was reduced by 68%, calcium by 39%, phosphorus by 30%, magnesium by 23%, chloride by 7%, and potassium by 6%. These reductions could be accounted for by the vegetative growth in the buffer. The authors recommended that riparian forest be used as nutrient filters to protect water quality and that selective harvesting of the hardwoods be done to insure a net nutrient uptake.

One of the considerations in developing buffer strips is the vegetation that will be used. Dillaha et al. (1985; 1989) observed that if the vegetation is unable to overcome sediment inundation by growth, the buffer will become ineffective. Research on the Edwards Plateau in Texas indicated that vegetation type also affects infiltration rates (Thurow et al., 1988). In general, the vegetation should have relatively rigid leaves, be taller than the expected depth of overland flow, and be able to withstand drought as well as inundation. The vegetation should be native if possible to prevent the changes in infiltration rates caused by disturbing the soil profile and compaction associated with landscaping activities (Kelling and Peterson, 1975). Several researchers found buffer strips to be ineffective when the flow depth is greater than the vegetation height (Dillaha et al., 1985; 1989; Tollner et al., 1976; Barfield et al., 1979; Hayes et al., 1979). In a study examining flow in vegetative channels, it was found that the vegetation remained rigid until the flow depth was greater than the height of the vegetation (Ree, 1949). Kao and Barfield (1978) found that, with a depth less than the

height of the vegetation, the vegetation drag was the dominant factor in flow retardation. When the depth of flow was greater than the height of the vegetation, the flow velocity increased greatly.

No field research has been conducted on the effectiveness of urban buffer strips. Field research focused on high concentrations of sediment and other pollutants. No research has been conducted on runoff with moderate to low concentrations of pollutants. Most of the research focused on constructed buffers not using native or adaptive vegetation in the buffer. These gaps in the research need to be filled before unqualified recommendations for the design of buffer strips can be made.

2.2 Buffer Strip Models

Overcash et al. (1981) developed a model for predicting pollutant reduction in buffers. They proposed that the major factors influencing buffer effectiveness were pollutant concentration, dilution by rainfall, and infiltration. Other factors included type of vegetation, settling, topography, and rainfall intensity. The model assumed that pollutants travel with the water, and the major mass loss of pollutant is by infiltration. This model does not take into account the effect of particles settling in the buffer strip. Development of this model was based on field research done by Bingham et al. (1980).

Most of the model development work has been done by a group of researchers at the University of Kentucky working on erosion control in surface mining areas (Barfield et al., 1979; Hayes et al., 1979; Kao and Barfield, 1978; Tollner et al., 1976; 1977). Tollner et al. (1976) presented design equations relating the fraction of sediment trapped in simulated, rigid vegetal material to flow depth, flow velocity, particle fall velocity, filter length, and vegetation density. This model was highly empirical and based on a theoretical number of times a particle could fall to the soil surface given certain flow conditions. Kao and Barfield (1978) performed experiments on different types of simulated vegetation to determine shallow flow hydraulics in vegetated waterways. They found that vegetation blade drag

is dominant in flows that have not topped the vegetation. This drag is proportional to the flow velocity squared and the depth of the submerged blade. Barfield et al. (1979), building on the previous work by this group, developed a steady state model, the Kentucky filter strip model, to determine the sediment trapping capacity of grass media as a function of slope, sediment load, flow velocity, flow duration, particle size, and media density. Outflow concentrations were found to be influenced mainly by slope and media density at a given flow velocity. Hayes et al. (1979) extended the Kentucky filter strip model to unsteady flow with non-homogeneous sediment. Methods were presented for determining hydraulic parameters required for real grasses. Model predictions were found to be in close correlation with laboratory plots for three types of grasses. This model has also been modified to predict phosphorous transport (Lee, 1987).

Flanagan et al. (1989) used the Chemicals, Runoff, and Erosion from Agricultural Management Systems (CREAMS) model (Knisel, 1980) for predicting sediment delivery through vegetative filter strips. It was determined that the CREAMS model, a field scale hydrologic model, satisfactorily predicted the sediment delivery through the filter strip. Simplified design equations based on the CREAMS methodology were also presented. These design equations yielded results similar to the complete CREAMS model. As with all other proposed buffer strip models, detachment of soil particles was not considered.

Phillips (1989) conducted research on hydraulic and detention models to determine the dominant factor in each model. The hydraulic model assumes the transport of pollutants in runoff through the buffer is directly proportional to the energy of the overland flow. This assumption is applicable to sediment, other large particles, and adsorbed pollutants. Subsurface flow is neglected. In the detention model, subsurface flow is taken into account and soluble pollutants play a major factor. The parameters studied were buffer width, hydraulic conductivity, Manning's n, slope, and soil moisture capacity. The hydraulic model was affected the most by variations in slope and hydraulic conductivity, with slope being dominant. The detention model was affected by buffer width and soil moisture capacity, with buffer width being dominant. The effect of varying Manning's n was the same for both

models.

3 Field Study

3.1 Site Description

A field study was conducted to develop a database related to water quality in an urban vegetative buffer to achieve the previously stated objectives. A site for the field study was selected in Austin, Texas. The runoff originated in a parking lot with a drainage area of approximately one hectare. The soil in the buffer zone was a Tarrent clay, a shallow to very shallow, well drained, stoney, clayey soil overlying limestone (United States Department of Agriculture, 1974). Some of the soil in the buffer was fill from the construction of the parking lot. The vegetation in the mowed and unmowed areas was primarily composed of Johnson grass (*Sorghum halepense*), Bermuda grass (*Cynodon dactylon*), and mixed legumes. The grassed buffer was followed by a wooded buffer dominated by common red cedar (*Juniperus virginiana*) with scattered live oak (*Quercus virginiana*) and Ashe juniper (*Juniperus ashei*). The ground cover was juniper litter and scattered Texas wintergrass (*Stipa leucotricha*).

3.2 Procedures

3.2.1 Data Collection

Test plots, areas with the same vegetation, were established to monitor the runoff quality through the buffer. Each plot was approximately 10 m by 20 m. The vegetation types included (1) grasses (3 replications), (2) grasses, mowed (3 replications), (3) undisturbed woodland (1 replication), and (4) cleared woodland (1 replication). Water samples were collected using a series of overland flow collection flumes, as shown in Figure 1, to route runoff into 1 liter sample bottles. The sample bottle was held in a 9 cm (4 in) diameter PVC tube to keep soil from surrounding the bottle and to make collection easier. A hole was drilled in the bottom of the tube to allow water to drain. Bolts were placed on both sides of the tube near the top. This allowed a rubber band to be placed over the top of the sample

bottle and 9 cm (4 in) funnel to keep them from floating in the sample tube. A 12.5 mm (1/2 in) spherical styrofoam float was placed in the sample bottle to keep excess sediment from entering the sample bottle once the bottle was full. The plastic spout at the end of the flume allowed the sample bottle to be removed without moving the flume. A cedar shingle cover flap at the end of the flume covered the sample collection bottle to prevent rainfall from entering the sample bottle. The cover flap was attached to the flume with a segment of nylon webbing, creating a hinge. A typical flume layout showing all components is shown in Figure 2.

Flumes were placed at four locations in the test plot: (1) at the entrance of the test plot, (2) one-third of the way into the test plot, (3) two-thirds of the way into the test plot, and (4) at the end of the test plot. In the cleared area, only three locations were used because of parkland restrictions on land clearing. Four flumes were placed at each sampling location, as shown in Figure 3. The slope of the test site was approximately 10% between location 1 (at the entrance of the test plot) and location 2 (one-third of the way into the plot) for the mowed and unmowed areas. Elsewhere, the slope was between 17 and 30%. The distance between locations was 4 m. The flumes collected runoff samples from twelve rainfall events on between July 1991 and October 1992. Sample bottles were placed in sample tubes only when a rainfall event greater than 10 mm was likely. This was done to reduce sample bottle contamination. Bottles were collected and sent for laboratory analyses if more than one half of the bottles were at least half full. If the bottles could not be collected for analysis within 36 hr of placement, they were emptied and cleaned.

3.2.2 Laboratory Analyses

The samples from three of the flumes at each location were analyzed by the City of Austin Water and Wastewater Laboratory for total suspended solids (TSS), total Kjeldahl nitrogen (T TKN), ammonia nitrogen (T NH_3–N), nitrate as nitrogen (T NO_3–N)), total phosphorus (T TP), total lead (Pb), and fecal coliforms (FC) using techniques approved by the U.S. Environmental Protection Agency (U.S. Environmental Protection Agency, 1979). When samples

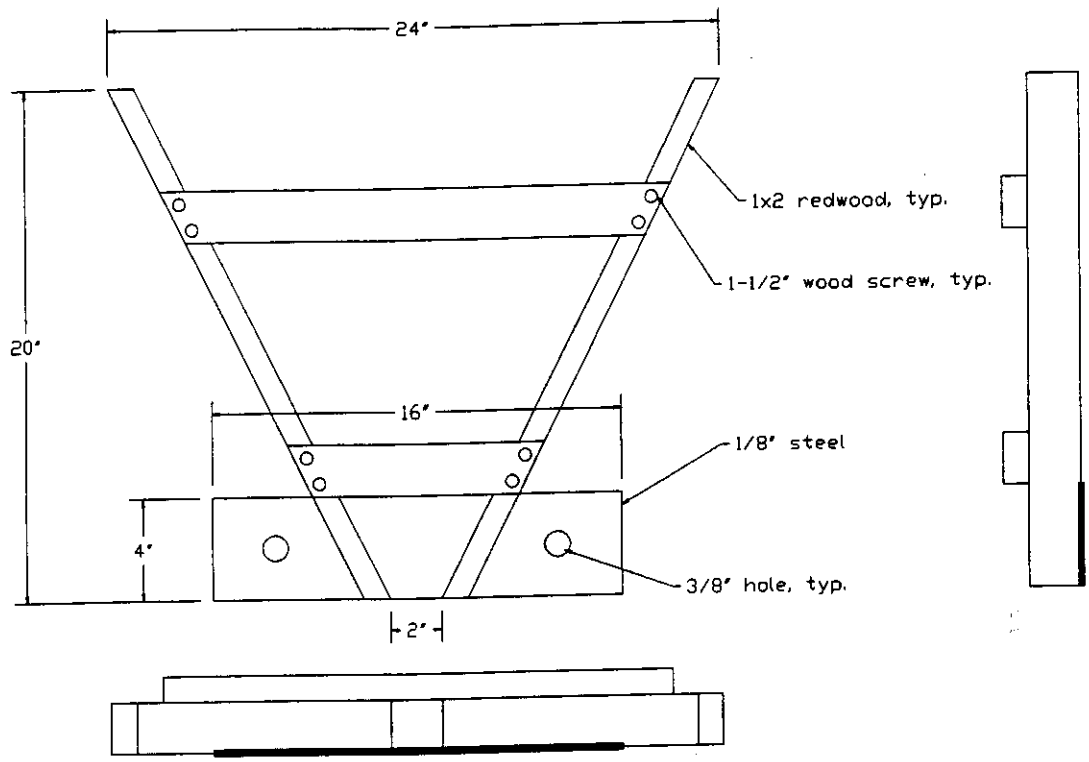

Figure 1: Collection flume.

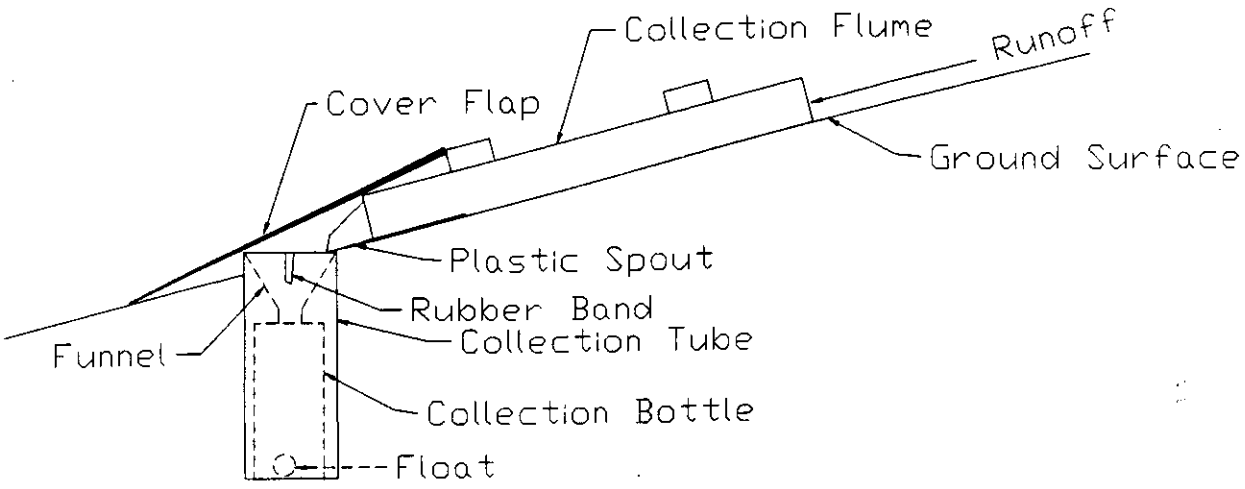

Figure 2: Collection flume and collection bottle layout.

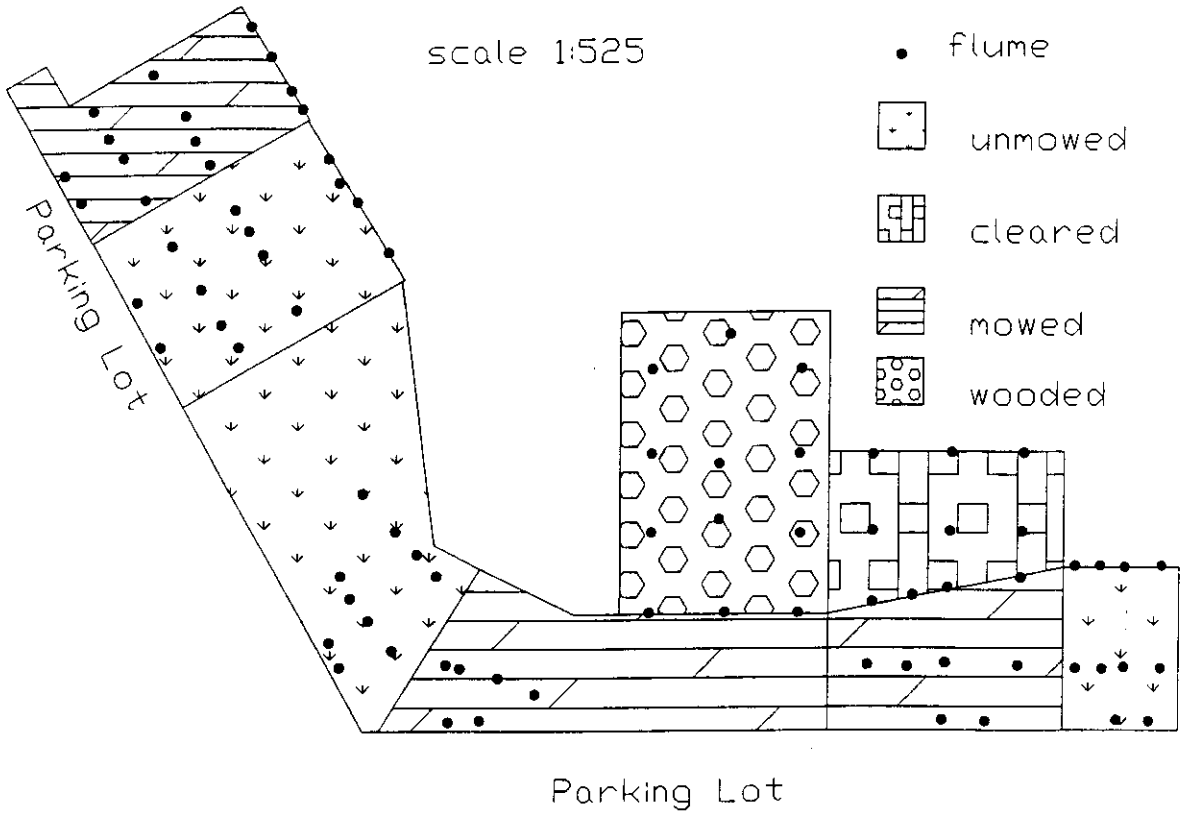

Figure 3: Test plot configuration.

could not be analyzed immediately, they were stored according to U.S. Environmental Protection Agency guidelines (U.S. Environmental Protection Agency, 1979). The fourth sample at each location was tested for dissolved ammonia nitrogen (D NH_3–N), dissolved nitrate as nitrogen (D NO_3–N), dissolved total Kjeldahl nitrogen (D TKN), dissolved total phosphorus (D TP), and fecal streptococci (FS). The prefixes T and D are used throughout this report to denote total and dissolved samples.

3.2.3 Infiltration

Infiltration characteristics were determined on adjacent areas with similar slope, soil, and vegetation as the buffer test plots. The infiltration test could not be conducted on the buffer test plots without disturbing the vegetation and flow characteristics in the buffer. A drip-type rainfall simulator (Blackburn et al., 1974) was used to produce runoff on plots averaging 0.345 m^2 in size. The simulated rainfall was applied at the rate of 15 cm/hr for one hour or until the final infiltration rate was reached, whichever was longer. The runoff was collected and weighed every five minutes. Infiltration was computed as the difference between the applied rainfall and the collected runoff. These data were used to determine the final infiltration rate. The infiltration test was repeated on each slope category and vegetation type, except the cleared area. The infiltration characteristics could not be determined on the cleared area because of limitations on the amount of land that could be cleared in the city park.

Two 75 mm diameter soil samples were collected from each infiltration test plot, one core at 0 to 25 mm and one at 25 to 50 mm. The soil samples were tested to determine soil texture by the particle size distribution method (Gee and Bauder, 1986), aggregate stability by the wet-sieve method (Kemper and Rosenau, 1986), soil organic matter content using the Walkley-Black technique (Nelson and Sommers, 1986), and bulk density by the core method (Blake and Hartge, 1986).

3.3 Results of Field Study

Water samples were collected from twelve rainfall events between July, 1990 and October, 1991. Four hundred twenty-five samples of the total pollutants and 125 samples for the dissolved pollutants were collected; some flumes did not collect samples on every event. The measured concentrations of all pollutant for each sample are included in Glick, 1992.

3.3.1 Statistical Analyses

Analyses of variance were conducted to determine the individual effects of vegetation composition and buffer width and the combined effect of the treatments on buffer effectiveness. Normality was tested to determine the validity of using the analysis of variance procedure. Treatment means were separated by Duncan's multiple range test. The statistical analyses were conducted using PC–SAS (SAS Institute Inc., 1988).

The dataset for each pollutant was tested for normality to determine the validity of using analysis of variance (ANOVA) techniques. It was determined by visual comparison that the concentrations were distributed log-normally for all datasets. By analyzing the natural log of the concentrations, the assumption of normality in the ANOVA procedure was not violated.

The statistical model used for the procedure included buffer width and vegetative cover as main effects and the interaction between the main effects. The complete SAS results are in Appendix A. For the total pollutants, only FC and T NH_3–N had models that were not significant at the 0.10 level. For these two pollutants, no significant trends or changes were determined in the data. Only D TP and D NO_3–N exhibited significant models among the dissolved pollutants.

The P–values, the probability that the means for the different treatments are equal, for individual model components for the pollutants with models significant at the 0.10 level are presented in Table 1. The values are based on the error for each term in the presence of all

Table 1: Analyses of variance results for pollutants with statistical models significant at the 0.10 level. Cover and buffer width are the treatments. Values indicate the probability that there is no difference in the means due to the given variables.

	Uncorrected P–Value		
Pollutant	Width	Cover	C×W
TSS	0.0001	0.0001	0.0457
Pb	0.0001	0.0001	0.0003
T TP	0.0163	0.0266	0.0355
T TKN	0.0431	0.0363	0.5596
T NO_3–N	0.4170	0.0055	0.0945
D TP	0.0001	0.4712	0.6314
D NO_3–N	0.4052	0.0004	0.6562

other terms in the statistical model, referred to by SAS as type III error (SAS Institute Inc., 1988). The interaction term was not significant for T TKN, D TP, and D NO_3–N. However, for parameters with a significant interaction term, the mean square error for the interaction must be substituted for the model mean square error to determine the corrected P–value for the main effects (Lentner and Bishop, 1986). The corrected P-value is used to determine if the interaction has masked any results such as significant main effects. The corrected P–values for the pollutants with significant interactions are in Table 2. Both the buffer width and cover had a significant impact on the concentrations of TSS and Pb. Using the corrected P–values, neither of the main effects for T TP or T NO_3–N were significant. For pollutants without a significant interaction, the analyses of variance procedure was performed again without the interaction term in the statistical model (Table 3). Vegetative cover was a significant factor at the 0.10 level for T TKN, D TP, and D NO_3–N. Only T TKN and D TP were significantly influenced by buffer width.

The mean concentrations for pollutants that showed a significant difference, at the 0.10 level, due to buffer width are given in Table 4. The mean concentrations for lead at 0 m

Table 2: Analyses of variance results for models with interactions significant at the 0.10 level. The p–value for the main effects has been corrected for the interaction.

	Corrected P–Value		
Pollutant	Width	Cover	C×W
TSS	0.029	0.033	0.0457
Pb	0.090	0.072	0.0003
T TP	0.478	0.529	0.0355
T NO_3–N	0.803	0.230	0.0945

Table 3: Analyses of variance results for models without significant interactions at the 0.10 level. The analyses of variance models have been changed to exclude the interaction term.

	Corrected P–Value	
Pollutant	Width	Cover
T TKN	0.0210	0.0850
D TP	0.0002	0.1057
D NO_3–N	0.3371	0.0001

Table 4: Means of sample concentrations for constituents with buffer width as a significant factor at the 0.10 level. Means in a row that do not have a letter in common differ significantly at the 0.05 level.

Pollutant	0 m	4 m	8 m	12 m
Pb ($\frac{mg}{l}$)	0.0166^b	0.0152^b	0.0230^a	0.0223^a
TSS ($\frac{mg}{l}$)	228.0^c	347.9^b	478.2^{ab}	612.8^a
T TKN ($\frac{mg}{l}$)	2.14^b	2.78^{ab}	3.25^a	3.32^a
D TP ($\frac{mg}{l}$)	0.184^b	0.320^a	0.440^a	0.438^a

Table 5: Means of sample concentrations for constituents with cover as a significant factor. Means in a row that do not have a letter in common differ significantly at the 0.05 level.

Pollutant	Mowed	Unmowed	Cleared	Wooded
Pb ($\frac{mg}{l}$)	0.0149^b	0.0173^b	0.0220^a	0.0261^a
TSS ($\frac{mg}{l}$)	331.0^b	321.2^b	383.0^b	630.2^a
T TKN ($\frac{mg}{l}$)	3.22^a	2.41^a	2.58^a	3.12^a
D TP ($\frac{mg}{l}$)	0.326^a	0.267^a	†	†
D NO_3–N ($\frac{mg}{l}$)	0.820^a	0.457^b	†	†

† Dissolved samples were not collected in the cleared or wooded areas due to space limitations.

and 4 m were significantly lower than the mean concentrations at 8 m and 12 m. The mean concentration of total suspended solids at the entry to the buffer was significantly lower than the concentration at all other locations. The mean concentration at 4 m was significantly lower than the concentration at 12 m. There was no significant difference between the concentrations at 4 m and 8 m and at 8 m and 12 m. The mean concentration at 0 m for total Kjeldahl nitrogen was significantly different from the concentrations at 8 m and 12 m. The mean concentration of dissolved total phosphorus at the entry was significantly lower than the concentrations at all other locations. The trend for all pollutants was for increasing pollutant concentration as the distance into the buffer increased.

Table 5 contains the mean concentrations for pollutants that showed significant differences due to the type of vegetative cover. Mean concentrations of lead were significantly higher for the cleared and wooded areas. The mean concentration of total suspended solids was significantly higher in the wooded area. There was no difference between the mean concentrations at the 0.05 level for total Kjeldahl nitrogen or dissolved total phosphorus. The mean concentration from the mowed area was significantly higher than the unmowed area for dissolved nitrate. Dissolved samples were taken only from the mowed and unmowed areas.

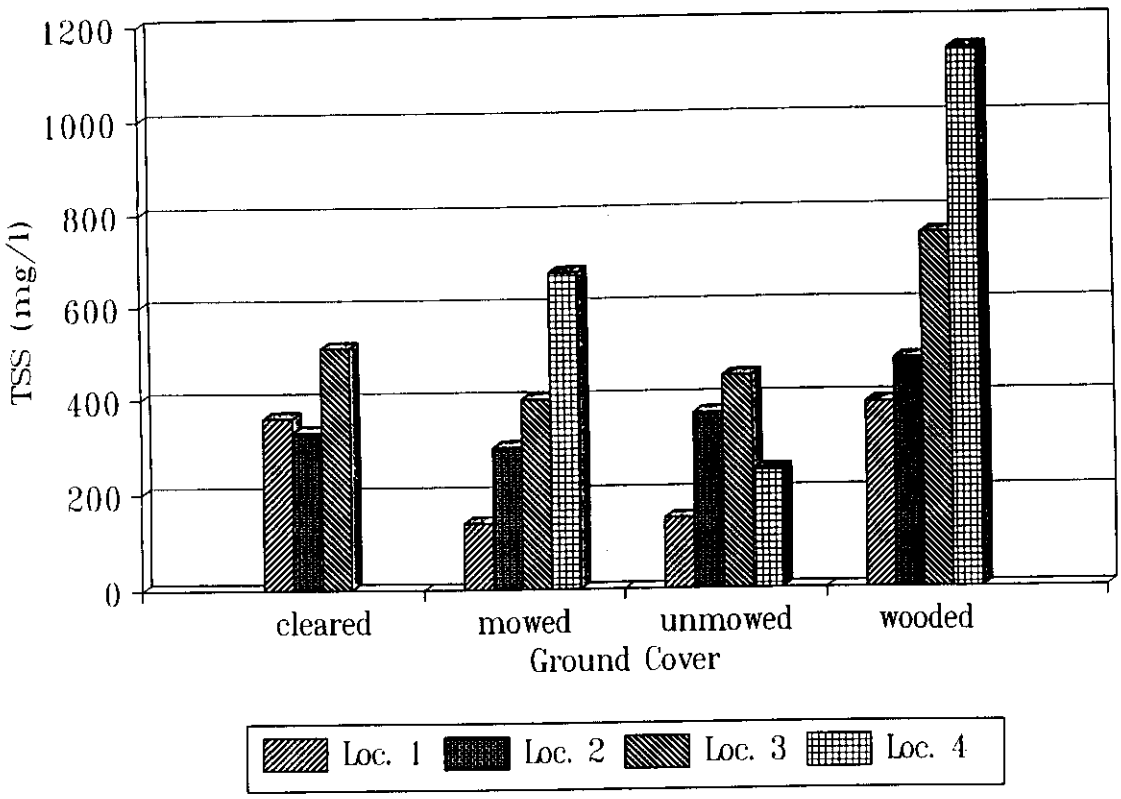

Figure 4: Total suspended solids. Mean concentration vs. buffer width with differences in vegetative cover.

Graphs showing the interaction for those pollutants with significant interactions are in Figures 4 through 7. The interaction between cover and buffer width for TSS (Figure 4) shows the mowed and wooded areas followed the same trend of increasing concentration, with the concentrations in the wooded area having a greater magnitude. This trend was also reflected in the data when looking only at buffer width. The concentrations in the unmowed areas increased until 8 m, then decreased. No trend could be observed for the concentrations in the cleared areas.

The interactions for lead are shown in Figure 5. As with TSS, in the wooded area, the concentration increased with increasing buffer width. In the cleared area, a large increase in concentration is noted between 4 m and 8 m, but no overall trend could be observed. The concentrations of lead in the samples from the mowed and unmowed areas varied slightly,

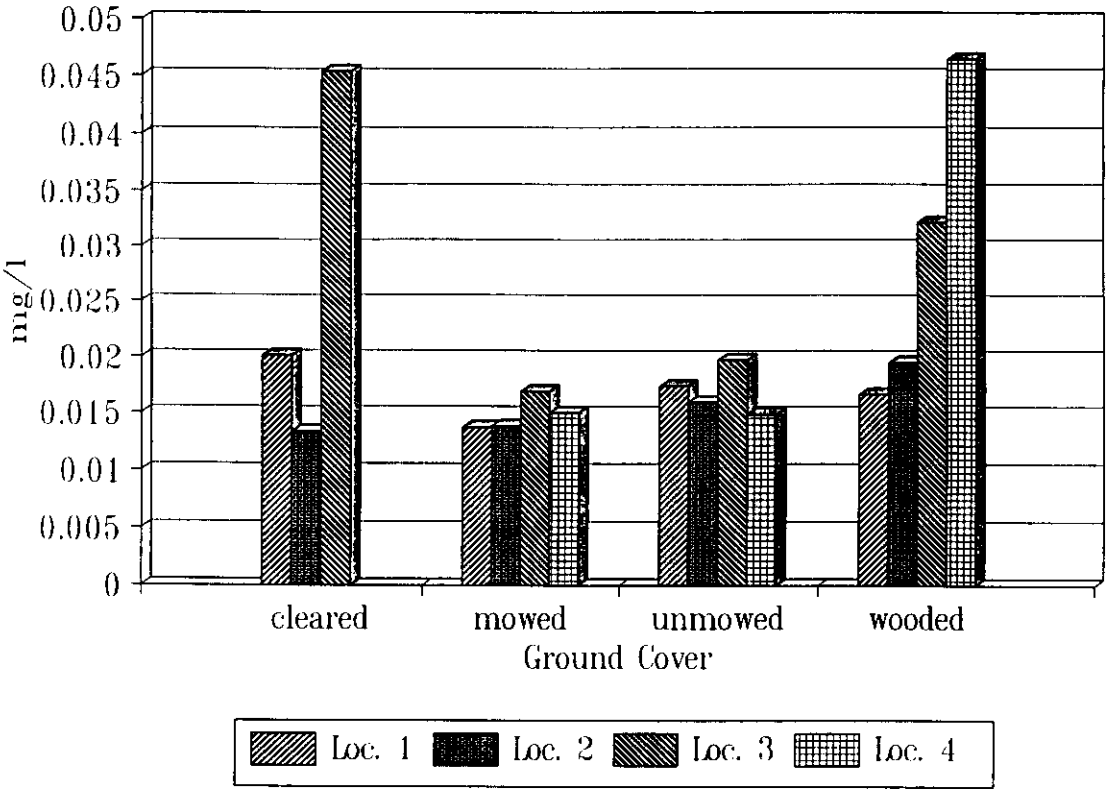

Figure 5: Total lead. Mean concentration vs. buffer width with differences in vegetative cover.

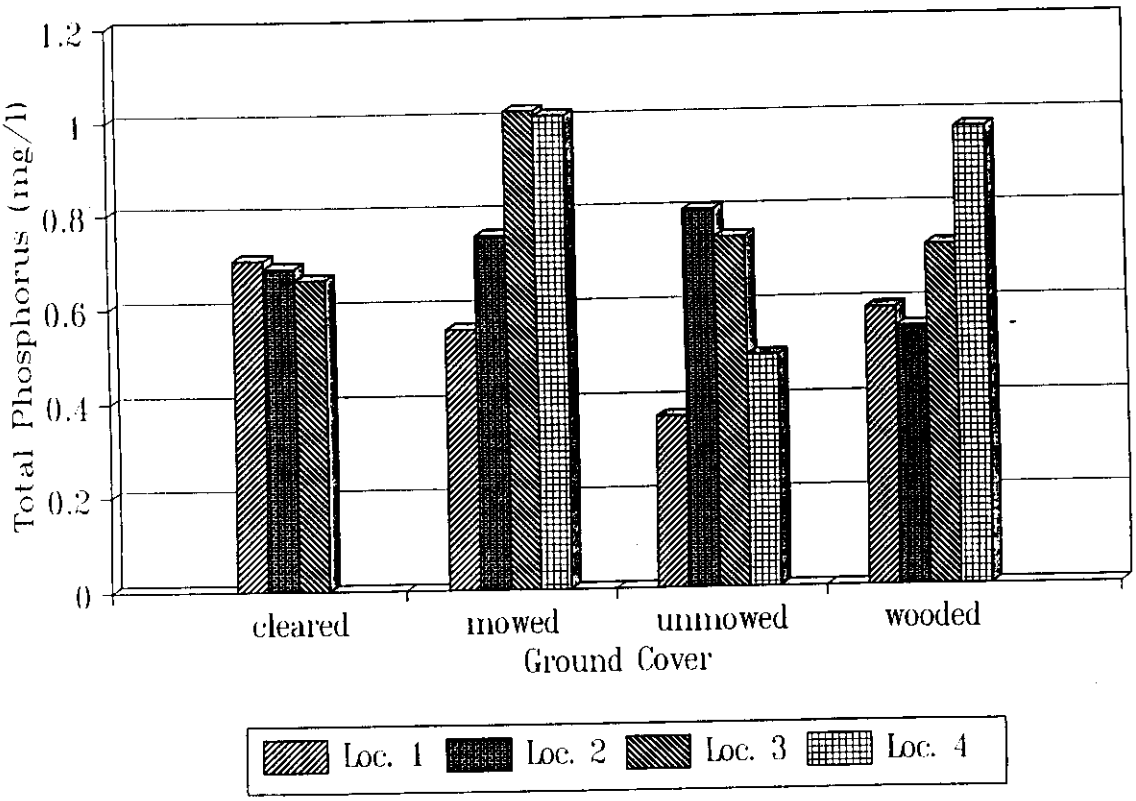

Figure 6: Total phosphorus. Mean concentration vs. buffer width with differences in vegetative cover.

but did not exhibit any trend. The concentration of lead was the same or greater at 12 m in each area when compared to the entering concentration of lead.

The concentrations of phosphorus in the mowed areas (Figure 6) increased between the buffer entry and 8 m before appearing to reach a constant level. In the unmowed areas, the concentration of phosphorus initially increased, then decreased. The concentration decreased slightly between the entry and 4 m in the wooded area, then increased. In all cases, except the cleared area, the final concentration was greater than the concentration entering the buffer.

The concentrations of total nitrate as nitrogen followed the same trend in all areas except the mowed areas (Figure 7). The general trend was for an increase, then a decrease to approximately the same concentration entering the area. The mowed area showed a significant

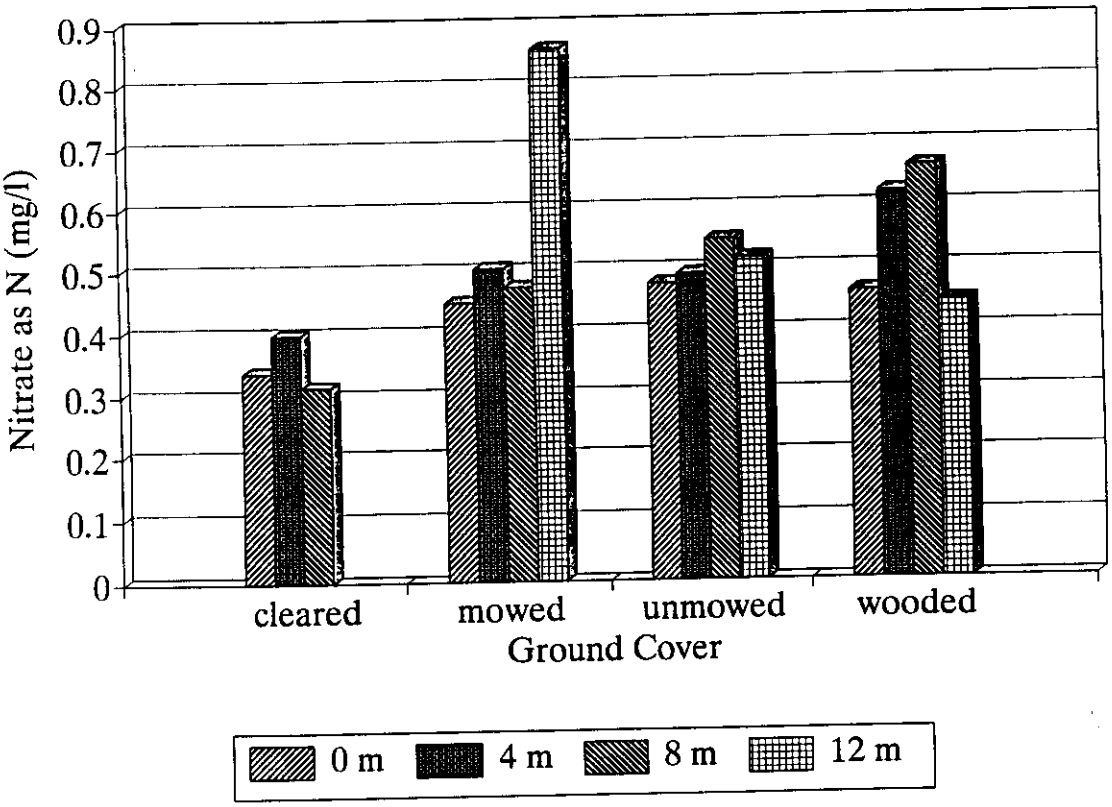

Figure 7: Total nitrate as nitrogen. Mean concentration vs. buffer width with differences in vegetative cover.

increase at the end of the buffer. The concentration of each pollutant entering the cleared and wooded areas is higher than the concentration entering the mowed and unmowed areas. This is due to the location of the cleared and wooded areas following 8 m of mowed buffer (Figure 3).

3.3.2 Infiltration

The results of the infiltration tests are shown in Figures 8 through 10. The results show that the mowed areas had final infiltration rates of 3 to 8 cm/hr, unmowed areas had infiltration rates of 11 to 14 cm/hr, and the wooded areas had infiltration rates greater than 14 cm/hr. The rainfall simulator applied 15 cm/hr.

The soil samples from 0-25 mm and 25-50 mm were tested for organic matter, aggregate stability, bulk density, and soil texture in the Watershed Management Laboratory in the Rangeland Ecology and Management department at Texas A&M. Average soil organic matter content for the mowed and unmowed areas was 2.9 and 2.3%, respectively. The organic matter content for the wooded area was 10.3%. The average aggregate stability was 27.25 and 32.13% in the mowed and unmowed areas and 81.55% in the wooded area. The average bulk density was 1.51, 1.43, and 0.96 gm/cm^3 in the mowed, unmowed, and wooded areas, respectively.

These results indicate that infiltration capacity and vegetative cover are highly correlated as shown in prior research (Dunne et al., 1988; Thurow et al., 1988). Areas with more dense groundcover tend to have higher infiltration rates for several reasons. One is the dissipation of the energy of the rainfall. The lowering of energy reduces the destruction of soil structure caused by rainfall impact. If the soil structure is destroyed, blocking of pores and lowering of the infiltration rate will generally occur. Secondly, examination of the soil data shows that organic matter, aggregate stability, and soil texture are related to vegetative cover. Each of these soil characteristics affect infiltration rates.

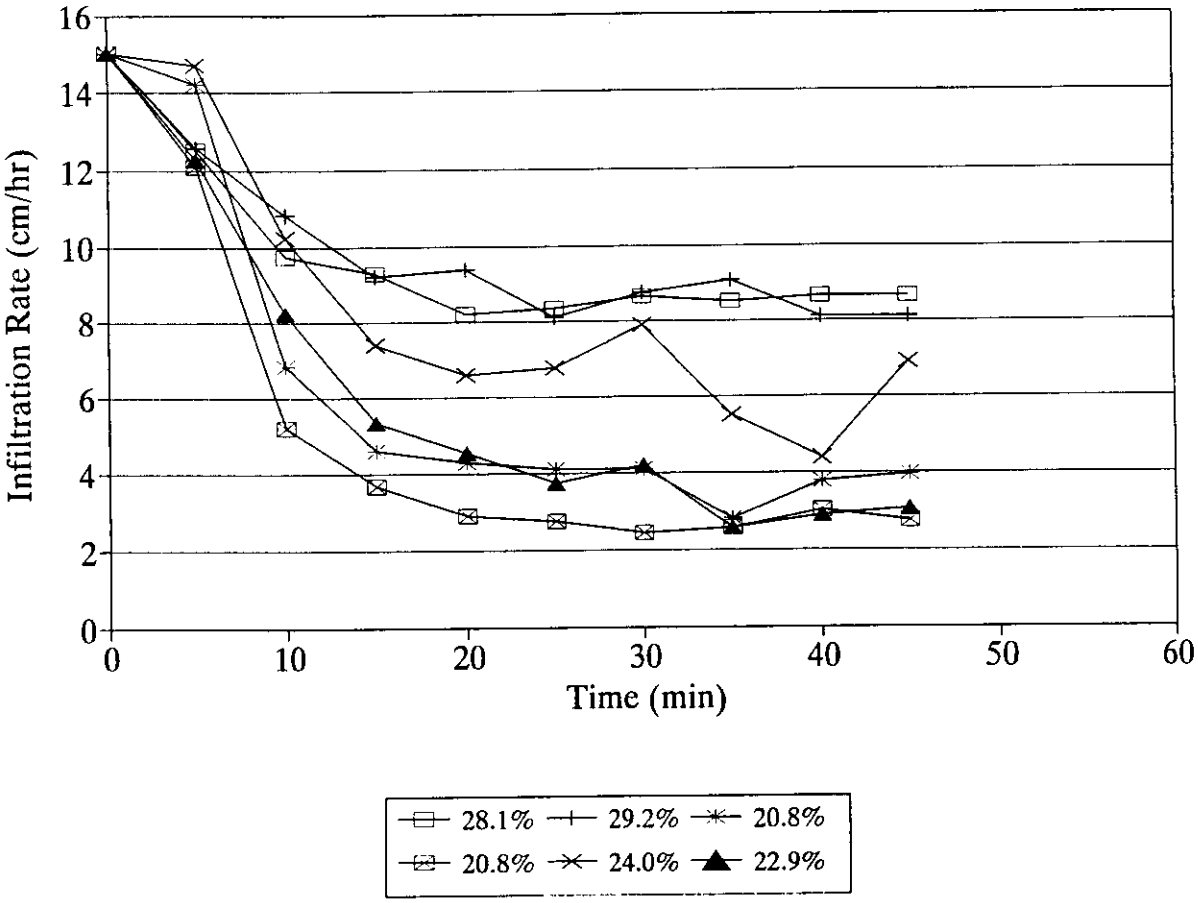

Figure 8: Results of infiltration tests on mowed areas. Infiltration rate vs. time with differences in slope for a single measurement.

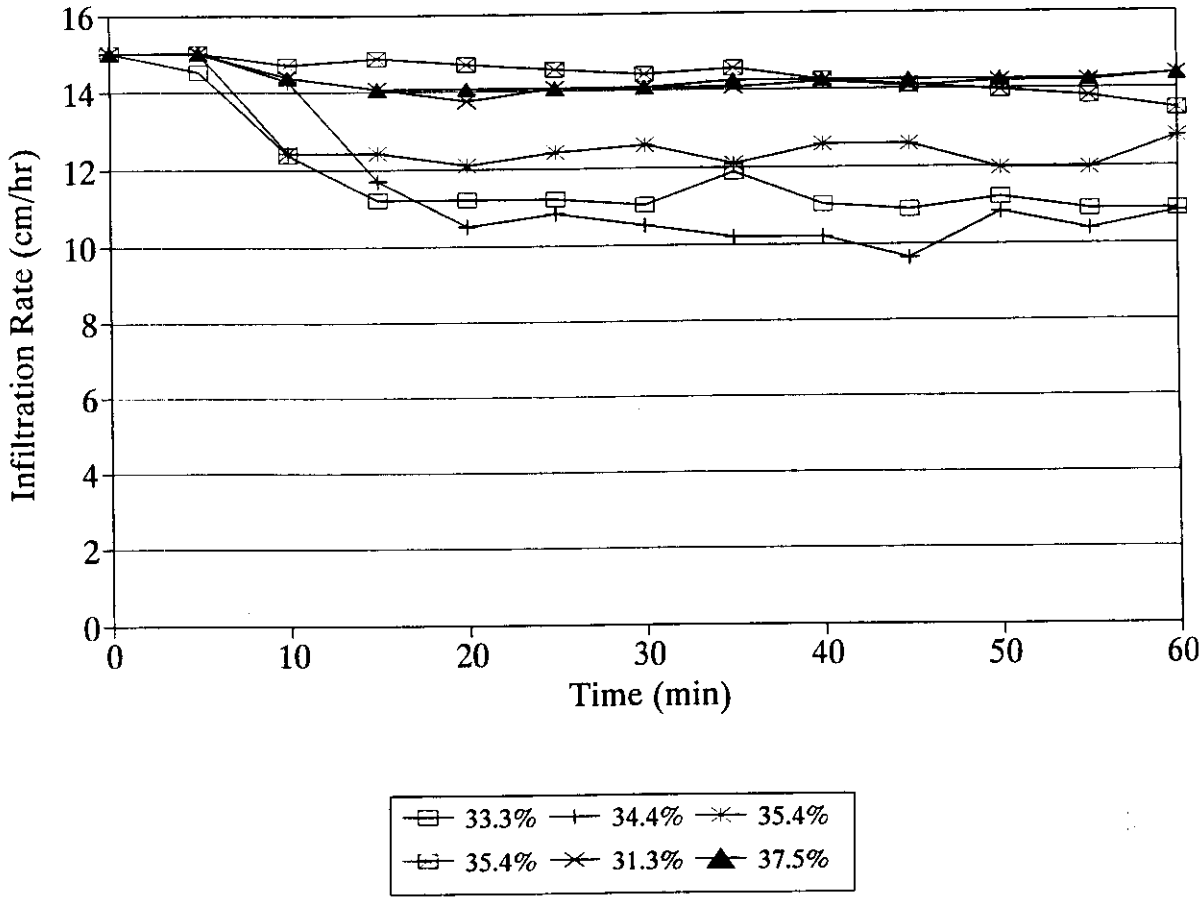

Figure 9: Results of infiltration tests on unmowed areas. Infiltration rate vs. time with differences in slope for a single measurement.

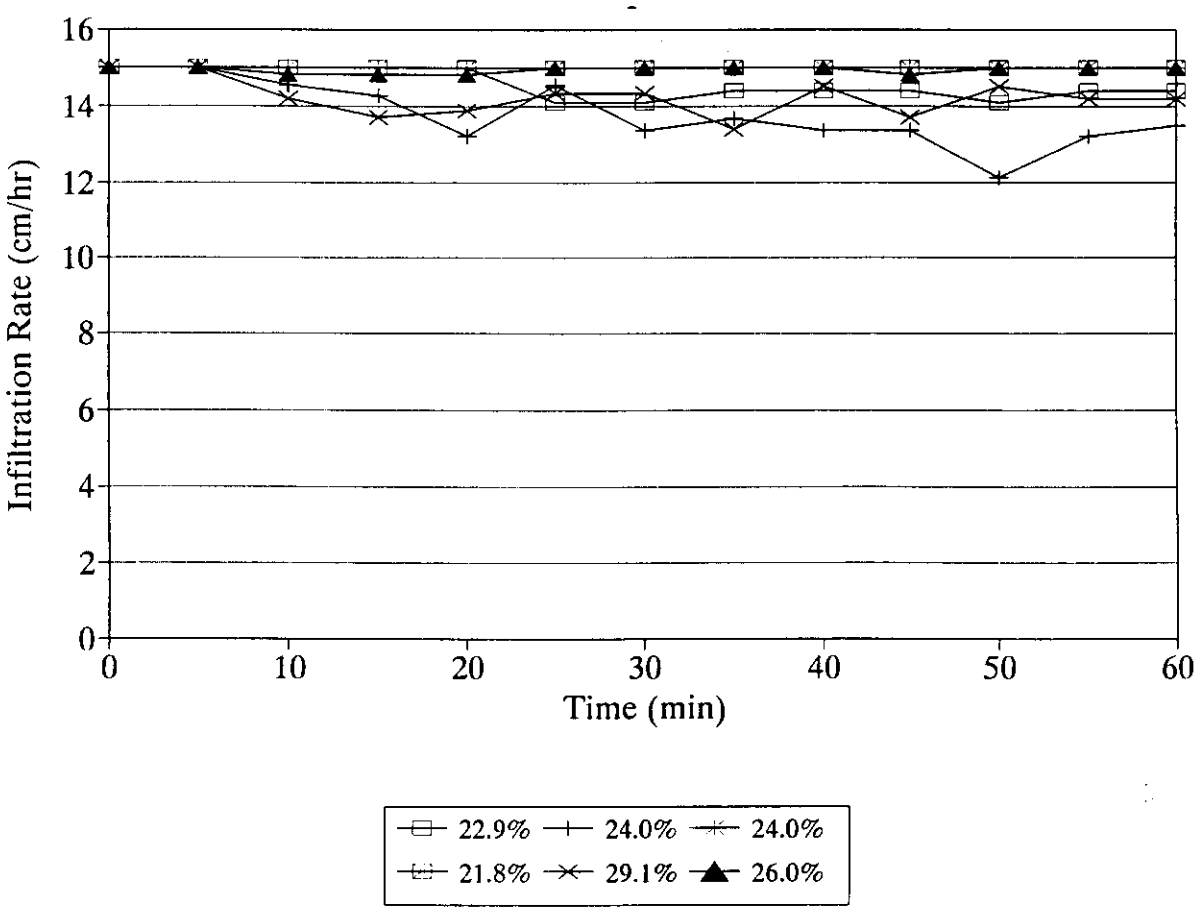

Figure 10: Results of infiltration tests on wooded areas. Infiltration rate vs. time with differences in slope for a single measurement.

3.4 Discussion of Field Results

Seven of the twelve pollutants tested in this study, TSS, Pb, T TP, T TKN, T NO_3, D TP, and D NO_3, exhibited a significant relationship between concentration and vegetative cover, buffer width or the interaction. Vegetative cover was a significant factor for five pollutants, Pb, TSS, T TKN, D TP, and D NO_3. The hypothesis that vegetative composition of the buffer influences its effectiveness is not rejected. For these pollutants, the wooded area showed a significantly higher mean pollutant concentration and the mowed and unmowed areas had generally lower concentrations. This may be due in part to the wooded and cleared areas being located downslope from the mowed and unmowed buffers. The groundcover on the wooded area is less dense than the groundcover in the mowed and unmowed area. Litter in wooded buffers was not considered because it tended to be washed away with the runoff. The groundcover in the wooded area did not reduce the rainfall impact energy as effectively as the grassed buffers, thus contributing to higher interrill erosion and a less effective buffer. From the collected data, it can be seen that the vegetative composition influences buffer strip performance.

Examination of the effective infiltration rates shows that the wooded area had the greatest infiltration rate, but the mean pollutant concentrations for total pollutants were also the highest. This does not support the hypothesis that as the infiltration rate of the soil in the buffer increases, buffer effectiveness increases. When comparing the mowed and unmowed areas which had similar vegetative cover, the mean concentrations were not statistically different but the unmowed areas had lower concentrations for four of the five pollutants. The unmowed area also had the higher infiltration rate. Comparing the dissolved pollutants, the unmowed areas had the lower mean concentration and the higher infiltration rate. This does support the hypothesis. It appears that infiltration rate is a secondary influence on buffer strip performance with the type of vegetation and ground cover being the primary factor. A higher infiltration rate would reduce the rill erosion and the transport in the interrill area and the vegetation reduces interrill erosion by rainfall. More research on the effects of infiltration rate on buffer strip effectiveness needs to be conducted.

Of the five pollutants that had buffer width as a significant factor, only dissolved nitrate had a lower concentration at the end of the buffer compared to the start. From this data, the hypothesis that as buffer width increases, its effectiveness increases is rejected. From the data gathered, it appears that buffer width negatively influences buffer performance. After an initial increase in pollutant concentration, the concentration tended to stabilize or increase slightly. This may be due to the low concentration of pollutant entering the buffer. If the runoff had a higher concentration of pollutants, then a decrease in pollutant concentration may have been observed. Dillaha et al. (1989) reported incoming total suspended solids of 4400 to 7500 mg/l and Doyle et al. (1977) reported concentrations of nitrogen and phosphorus of 47.0 and 21.23 mg/l, respectively. Those field studies were performed in agricultural settings and reported decreasing concentrations as buffer width increased. However, the concentrations leaving the buffer in the agricultural studies were equal to or greater than the concentrations leaving the buffer in this study. The "clean" runoff contributes to an excess in transport capacity when entering the buffer. If the buffers studied were longer, then a decrease from the peak concentration may be observed. This may be seen in the data as the slight decrease in pollutant concentrations between 8 m and 12 m. The vegetation in the buffer can increase nutrient loads by the contribution of dead plant matter. The nutrient levels observed leaving the buffer in this field study were not unlike those expected from runoff from a natural grassland.

The effects of changing slope are inconclusive. The slope of the buffer changed at 4 m in the mowed and unmowed areas. Comparing the change in concentration between 0 and 4 m and between 4 and 8 m, the differences were not significant. If the slope had remained constant, a decrease in pollutant concentration may have been observed with this buffer width. This change in slope may be a major factor in the continued increase in pollutant concentrations.

Comparing the concentrations of total and dissolved pollutants, it can be seen that the concentrations of the total pollutants are two to three times higher than the concentrations of the dissolved pollutants. This leads to the conclusion that a large portion of the pollutants are

adsorbed on the sediment and pollutant concentrations are linked to sediment concentrations.

The effects of dry deposition and deposition by rainfall in the buffer were not a part of this study, but their impact may be significant. The concentrations that are not significant, FC, FS, T NH_3, D NH_3–N, and D TKN, are for constituents that would not be found in dry deposition or deposition by rainfall. In an urban environment, air borne pollutants and dust, generally, are found in higher concentrations than in rural areas. Because the pollutants are deposited on the vegetation and directly on the ground, they can become entrained in runoff. The effects of dry deposition need to be studied and addressed in urban and rural buffer strip studies.

Both pollutant concentrations and mass loadings are important. In this study, only the concentrations of the runoff were measured. Past studies (Doyle et al., 1977; Neibling and Alberts, 1979; Bingham et al., 1980; Dillaha et al., 1989) have examined both pollutant concentration and mass loading. Measurements of the flow volume needed to compute the loadings were not available as originally planned in this study due to logistical difficulties encountered by the City of Austin. The total mass loading of pollutants may have decreased due to infiltration reducing total runoff, but the concentration increased. This area needs further study.

Drinking water and other (e.g., contact, agriculture) standards have been set for some of the measured pollutants (United States Environmental Protection Agency, 1990). Only lead and bacteria exceeded the standards. The average concentration of lead leaving the buffer was 0.0223 mg/l with the drinking water standard being 0.015 mg/l. The bacteria drinking water standard is zero with a contact level of 200 colonies per 100 ml. Fecal streptococci had an average level of 49365 colonies per 100 ml and fecal coliforms had an average level of 1701 colonies per 100 ml. The drinking water standard for nitrate and total nitrogen is 10 mg/l as nitrogen. The concentration of TKN leaving the buffer was 3.32 mg/l and the concentration of D NO_3 was 0.259 mg/l, both below the EPA drinking water standards.

4 Buffer Strip Modeling

Several models have been developed to predict the effectiveness of vegetative buffer strips (Bingham et al., 1980; Barfield et al., 1979; Flanagan et al. 1989; Lee, 1987). None of these models are directly applicable to the urban scenario studied here because the models do not include the process of soil detachment in the buffer strip. The results of the field study indicate that detachment does occur in the buffer strip. A physically-based, process oriented model that does allow for detachment in the buffer strip as well as deposition was developed to simulate this situation. The model only simulates sediment production because more is known about the processes governing sediment detachment and deposition compared to the other pollutants studied. The field study also indicated, by comparing concentrations of dissolved and total pollutants, that the adsorbed portion of pollutants is two to three times higher than the dissolved portion and is closely linked to the concentration of sediment.

4.1 Model Development

The buffer strip model was developed using components previously validated by other researchers and in wide use to simulate the various hydrologic processes acting on the flow through the buffer strip. The model has four main components:

1. Inflow Concentration Simulator,
2. Surface Runoff and Routing,
3. Detachment/Deposition, and
4. Transport.

These components simulated the buffer strip for a single runoff event and allow the concentration of sediment entering the buffer to vary statistically. A listing of the program is included in Appendix B.

4.1.1 Inflow Concentration Simulator

The inflow concentration simulator takes into account the variability of the inflow concentration. As seen in the field study, the data were distributed log-normally. The mean and standard deviation of the log of the concentration of sediment entering the buffer are inputs to the model. The inflow concentration is approximated stochastically using this information and provides the natural variability found in the field study. The inflow for only the mowed and unmowed buffers were used to determine the statistical characteristics of the model inflow.

The inverse transformation approach (Law and Kelton, 1982) was used to generate the inflow concentration. This approach consists of two steps. First, a uniform random number generator generates a number, U, from the U(0,1) distribution. Then, using the inverse of the distribution function, let $X = F^{-1}(U)$, where X is the incoming sediment concentration.

The model uses a prime modulus multiplicative linear congruential generator (PMMLCG) to generate random numbers. The random number generator is defined by:

$$Z_i = (7^5 Z_{i-1}) \pmod{2^{31} - 1} \tag{1}$$

This PMMLCG has been tested and is used widely (Law and Kelton, 1982).

4.1.2 Overland Flow

The first theoretical equations put forth to predict overland flow are attributed to Barre de St. Venant (Huggins and Burney, 1982). The hydrodynamic equations proposed by St. Venant depend on the conservation of linear momentum and the conservation of mass. These equations have no closed form, but have been solved graphically in some cases. This approach has become outdated with the use of computers and numerical techniques.

Lighthill and Whitham (1955) proposed that the dynamic term in the momentum equation could be omitted if backwater effects were not present. The resulting equation is the

kinematic wave equation. The depth of overland flow and the rate of discharge per unit width are computed for using the following equations (Huggins and Burney, 1982):

$$\frac{\partial Y}{\partial X}dX + \frac{\partial Y}{\partial t}dt = dY \tag{2}$$

and

$$\frac{\partial Q}{\partial X}dX + \frac{\partial Q}{\partial t}dt = dQ \tag{3}$$

Solving these equations simultaneously yields:

$$Y_{(X,t)} = Y_{(X,t-\Delta t)} - \frac{\Delta t}{\Delta X}(Q_{(X,t-\Delta t)} - Q_{(X-\Delta X,t-\Delta t)}) + RE\Delta t \tag{4}$$

Several methods may be used to compute $Q_{(X,t)}$. The model uses Manning's equation defined by:

$$Q_{(X,t)} = S^{\frac{1}{2}}\frac{K}{n}Y^{\frac{5}{3}}_{(X,t)} \tag{5}$$

where,

Y=flow depth, L,
Q=discharge per unit width, $L^3/T/L$,
RE=rainfall excess, L/T,
X=position down slope, L,
ΔX=position increment, L,
t=time from the beginning of the event, T,
Δt=time increment, T,
S=slope of the flow plane, decimal,
n=Manning's roughness coefficient,
K=1.49 for English units and 1.0 for SI units.

Woolhiser and Ligget (1967) studied the effect of omitting the dynamic effects from the momentum equation. It was found that the effects could be evaluated by:

$$k = \frac{S_o L}{HF^2} \tag{6}$$

where,

S_o = slope of the flow plane at the outlet, decimal,

L = length of the bed slope, L,

H = equilibrium flow depth at the outlet, L,

F = equilibrium Froude number for the outlet, dimensionless.

If k is greater than 10, very little accuracy is lost by neglecting the dynamic effects. In almost all overland flow cases, including those in this study, k is greater than 10.

Rainfall excess is computed as the difference between the potential depth of infiltration and the depth of rainfall during a given time step. If rainfall excess is negative, runoff is allowed to infiltrate to simulate transmission losses. The infiltration rate is computed at each time step. The infiltration component of the model utilizes the equations developed by Green and Ampt (1911). Based on Darcy's law, the Green and Ampt model approximates potential infiltration using the soil's physical properties. Infiltrating water is conceptualized as a wave front entering the surface and saturating the soil as it progresses deeper into the soil profile.

Cumulative infiltration is computed as a function of the soil's water holding capacity, soil moisture suction, hydraulic conductivity and depth of surface ponding. The relationship is shown below in this form of the Green and Ampt equation (Chow et al., 1988):

$$F(t) = Kt + (\Psi + h_o)\Delta\Theta \ln\left(1 + \frac{F(t)}{(\Psi + h_o)\Delta\Theta}\right) \tag{7}$$

where,

$F(t)$ = Cumulative infiltration at time t, L,

K = hydraulic conductivity, L/T,

t = cumulative time, T

Ψ = soil moisture suction at the wetting front, L,

h_o = depth of ponding on soil surface, L,

$\Delta\Theta$ = effective soil moisture holding capacity, L.

In the buffer strip model, infiltration rate is solved for iteratively using the cumulative infiltration from the previous time step using the following equation (Chow et al., 1988):

$$f(t) = K\left(\frac{(\Psi + h_o)\Delta\Theta}{F(t)} + 1\right) \tag{8}$$

where,

$f(t)$ = infiltration rate at time t, L/T.

The values obtained for cumulative infiltration and infiltration rate represent the maximum potential values for that time step. The actual values may be less if there is no rainfall or overland flow from upstream. The model sets the infiltration rate at the maximum allowable after verifying rainfall or overland flow is present.

The model requires a hydrograph of the runoff entering the buffer. Since this was not available, the entering hydrograph was simulated for each storm. The hydrograph was simulated using the kinematic wave technique and the parameters of the area where the runoff originated.

4.1.3 Detachment/Deposition

The detachment component of the model uses a modified Universal Soil Loss Equation (USLE) as developed by Foster et al. (1977). This is the same method that is used in the CREAMS model (Knisel, 1980). The CREAMS model could not be used directly because it does not allow for the input of runoff into the area that is being simulated. The ability to input runoff from contributing areas is important because, in many cases, the characteristics of the buffer and contributing areas are dissimilar. The interrill and rill detachment processes are described by the following equations:

$$D_{Li} = 0.210\ EI\ (s + 0.014)\ KCP\ \frac{\sigma_p}{V_u} \tag{9}$$

and

$$D_{Fr} = 37983\ mV_u\sigma_p^{\frac{1}{3}}\ \left(\frac{x}{72.6}\right)^{m-1} s^2\ KCP\ \frac{\sigma_p}{V_u} \tag{10}$$

where,

D_{Li} = interrill detachment rate (lb/ft^2/s),
D_{Fr} = rill detachment capacity rate (lb/ft^2/s),
EI = Wischmeier's rainfall erosivity,
x = distance down slope (ft),
s = sine of the slope angle,
m = slope length exponent,
K = USLE soil erodibility factor,
C = USLE cover-management factor,
P = USLE contouring factor,
V_u = runoff volume (volume/unit area),
σ_p = peak runoff rate (volume/unit area/unit time).

The modified USLE used in the CREAMS model was developed using English units. The constants in the model were developed using regression with English units and have not been developed and validated using SI units. The buffer strip model converts SI units of the inputs to the needed English units and converts the results of the modified USLE to SI units.

Rainfall erosivity (EI) is the main component in determining the interrill detachment rate. The erosivity is found by the equation:

$$EI = 8.0\ V_R^{1.51} \tag{11}$$

where V_R is the depth of rainfall in inches. This approximation, outlined in the CREAMS user manual (Knisel, 1980), was developed from data points used in the development of the USLE and has a coefficient of determination of 0.56. V_R is a required input depending on the storm being simulated.

The slope length exponent (m) is set at 2, which is accurate for buffers less than 45.72 m (150 ft) wide (Knisel, 1980). The input values for the USLE factors (K, C, and P) are determined from published tables and graphs used with the USLE. The runoff parameters (σ_p and V_u) are computed in the surface runoff component of the model.

4.1.4 Transport Capacity

Several equations have been developed to predict transport capacity. The equation used in this model for overland flow and nonuniform sediment was developed by Yalin (1963) and modified by Foster and Meyer (1972). The dimensionally homogeneous equation is:

$$\frac{W_s}{SG\rho_w dV_* g} = 0.635\ \delta\ [1 - \frac{1}{\sigma} Ln(1+\sigma)] \tag{12}$$

where,

$\sigma = A\delta$

$\delta = \frac{Y}{Y_{cr}} - 1$ (when $Y < Y_{cr}$, $\delta = 0$)

$A = 2.45\ SG^{-0.4} Y_{cr}^{0.5}$

$Y = \frac{V_*^2}{(SG-1.0)gd}$

$V_* = (gRS_l)^{0.5}$ or

$V_* = \sqrt{\frac{\tau}{\rho_w}}$

and

W_s = transport capacity (mass/unit width/unit time)

V_* = shear velocity

τ = shear stress

g = acceleration of gravity

ρ_w = mass density of the transporting fluid

d = particle diameter

Y_{cr} = critical lift force given by the Shield's diagram extended to low particle Reynolds numbers

R = hydraulic radius
S_l = slope of the energy grade line
SG = particle specific gravity.

The Yalin equation was originally developed for transport of particles of uniform size. Foster and Meyer (1972) modified the equation for a mixture of particle sizes by reducing the number, but not the velocity, of particles of a specific size. Yalin assumed the number of particles in transport to be proportional to δ. For a given particle size, i, the number of particles in transport is proportional to δ_i. All values of δ_i are computed and summed giving:

$$T = \sum_{i=1}^{n} \delta_i \tag{13}$$

where n is the number of particle size groups.

Letting the left side of Equation (12) equal P, then:

$$(P_e)_i = \frac{P_i \delta_i}{T} \tag{14}$$

where $(P_e)_i$ is the effective P for size i in a mixture.

The actual transport capacity for particles of size i, W_{si}, can then be calculated by:

$$W_{si} = (P_e)_i \; SG \; \rho_w g d V_* \tag{15}$$

The total transport capacity can be found by:

$$W_s = \sum_{i=1}^{n} W_{si} \tag{16}$$

assuming there is an excess of each particle size to be transported.

To compute the shear velocity, V_*, the model uses the formula using τ and ρ_w rather than estimating the hydraulic radius. Using the methodology from CREAMS (Knisel, 1980), the total shear stress, τ, is divided between the shear stress acting on the soil, τ_s, and the stress

acting on the vegetative cover, τ_v. The portion of the stress acting on the soil, used to compute the shear velocity, is found by:

$$\tau_s = \gamma\ ys \left(\frac{n_{bs}}{n_{cov}}\right)^{0.9} \tag{17}$$

where,

γ = weight density of water

y = flow depth for smooth, bare soil

s = sine of the slope angle

n_{bs} = Manning's friction factor for bare soil (set at 0.01)

n_{cov} = total Manning's friction factor including vegetation.

The bare soil flow depth is computed by:

$$y = \left(q_w \frac{n_{bs}}{s^{0.5}}\right)^{0.6} \tag{18}$$

where q_w is the rate of discharge per unit width.

4.2 Model Input

The input may be divided into two main categories, buffer data and rainfall data. The buffer data include the segment slope, the segment length, hydraulic conductivity, soil moisture suction, soil moisture holding capacity, Manning's roughness factor, the USLE factors K, C, and P, and the soil particle distribution. The model currently sets the number of segments at three. Rainfall data needed for the model operation are the length of the simulated runoff event, time increments for simulation, total rainfall depth, the incoming runoff hydrograph expressed as depth of flow per time increment, the maximum incoming runoff rate, the maximum incoming runoff depth, and the total incoming runoff. Several items do not fit into either category. These items are the log of the mean concentration of incoming sediment distribution and the standard deviation of the incoming sediment distribution. The mass

density of water, data points for the Shields diagram, and the acceleration of gravity are contained in the data file.

4.3 Model Output

The model was tested using data from five storms for which field data were collected. Rainfall and a simulated runoff hydrograph were the variable inputs for each storm. A simulated hydrograph is used as an input to the buffer because flow rates were not collected entering the buffer. The hydrograph was produced using the kinematic wave method on the parking lot. The five storms were simulated ten times each. Multiple simulations were performed to account for the variability of incoming sediment concentrations in each storm. Only mowed and unmowed buffers were simulated. The results of the multiple simulations for each storm were averaged to yield one concentration for each cover, location, and storm, resulting in forty values. The results of these simulations are compared with the field data in Figure 11.

The results of the model fall into two categories, either the model overpredicted sediment concentrations or the model predicted a zero concentration of sediment when there was a measured concentration. The cases where the model predicted a zero concentration are found, for the most part, in the storms on 21FEB91 and 16MAR91. These storms had low rainfall and the model predicted that all the runoff would be lost through transmission losses. The model predicted the concentration of sediment based on the peak runoff rate, however, the field data were collected from the initial runoff. If the peak runoff rate was not at the beginning of the event, the model would overpredict as seen.

The concentration for each buffer width and cover were averaged to determine long-term trend predictions. These results are shown in Figure 12. The averages of the concentrations for the simulated buffer do not include cases where the model predicted a zero concentration. This was done to be consistent with the collected field data. If a sample was not collected from a flume in the field study it was not included in the average, therefore, if the model predicted

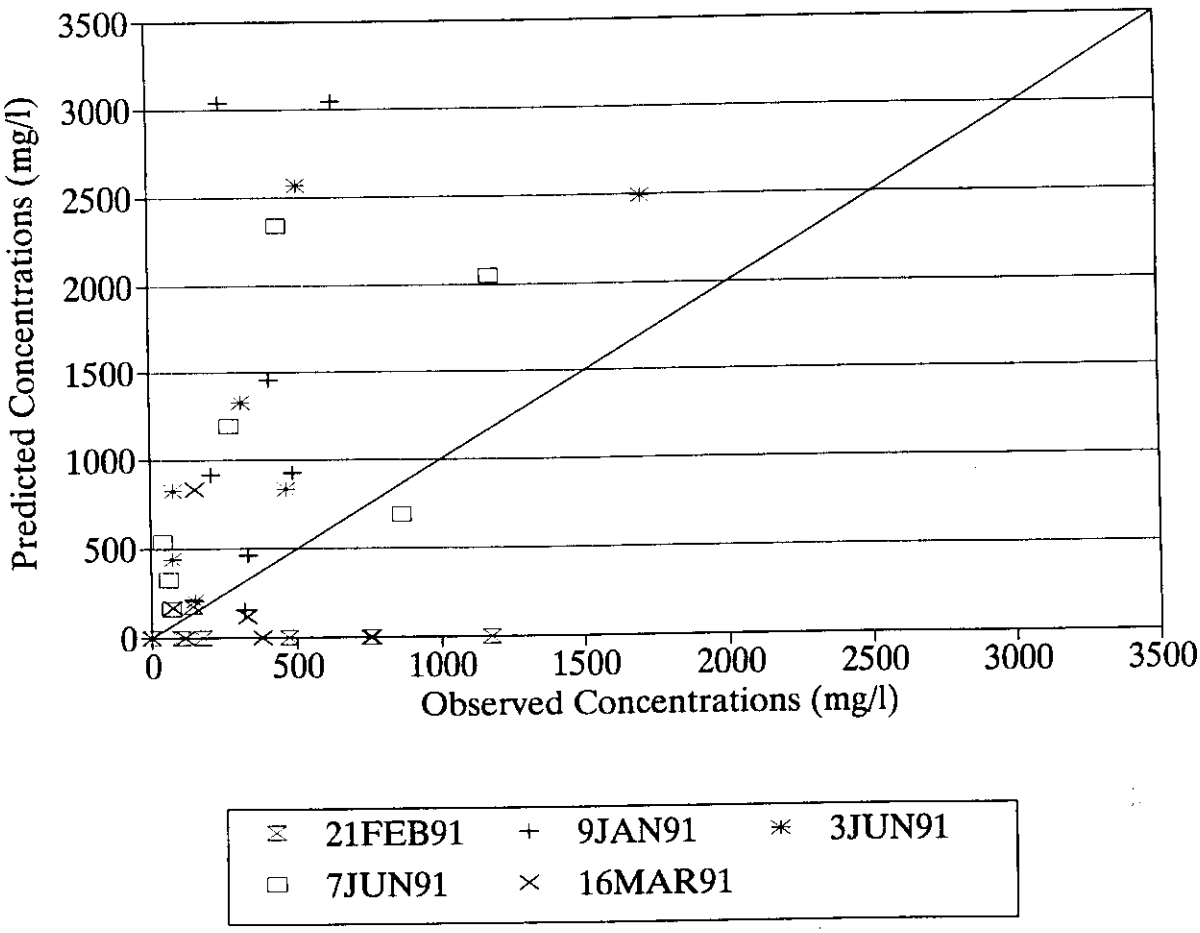

Figure 11: Predicted concentrations of total suspended solids vs. actual concentrations of total suspended solids for five events.

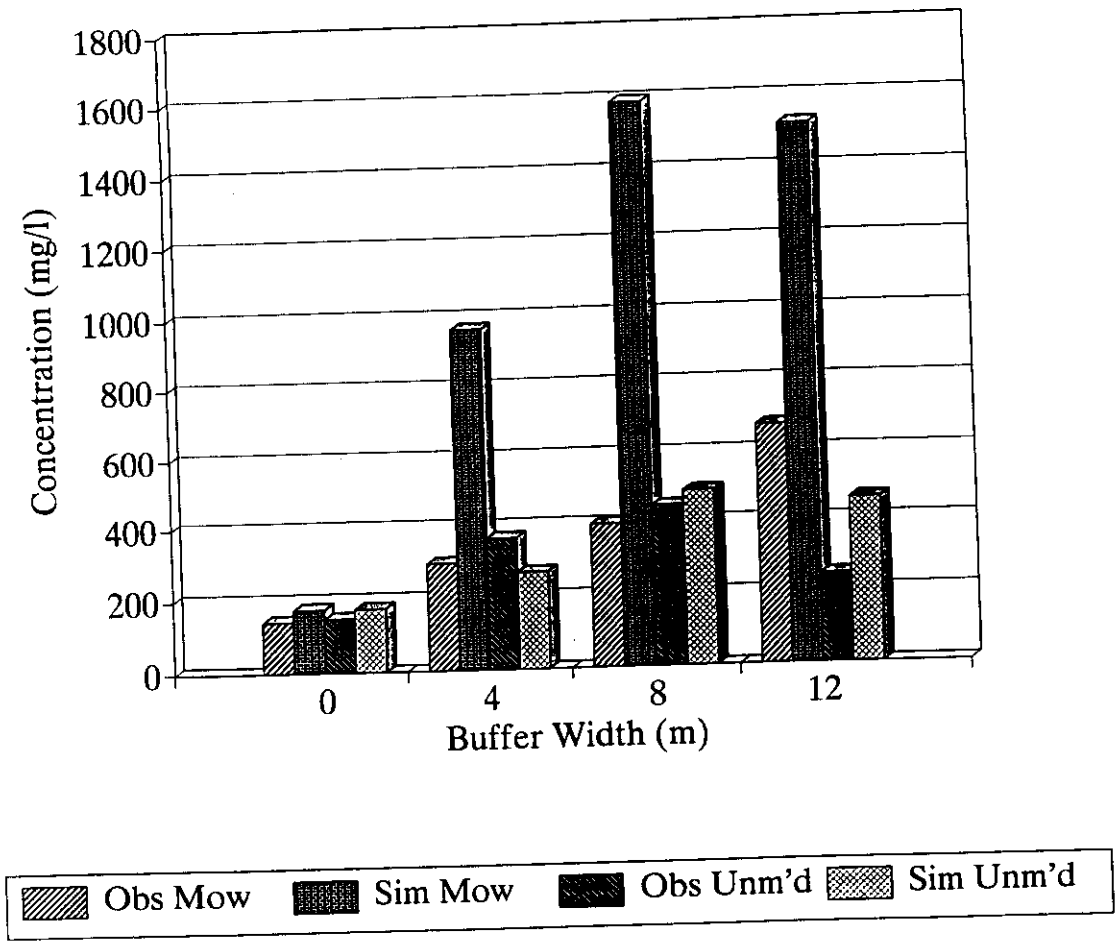

Figure 12: Total suspended solids concentration vs. buffer width. Simulated and field data are shown.

no sediment because of no runoff then that value should be excluded. The simulated average concentrations at the entrance to the buffer were very close to the field data. At 4 m into the buffer, the simulation predicted closely the concentration of TSS for the unmowed buffer. The model overpredicted the concentrations for the mowed buffer at 4 m, as well as at other locations in the buffer. At 8 m into the buffer, the model overpredicted the concentration for the mowed buffer, but closely predicted the concentration for the unmowed buffer. At the end of the buffer, the model reasonably predicted the concentration of TSS in the unmowed buffer but overpredicted the concentration of TSS in the mowed buffer. The decrease in concentration of TSS in the unmowed buffer was predicted. In all cases transport capacity, not detachment/deposition, controlled the TSS concentration.

To test this model for other applications where the concentration of sediment decreases,

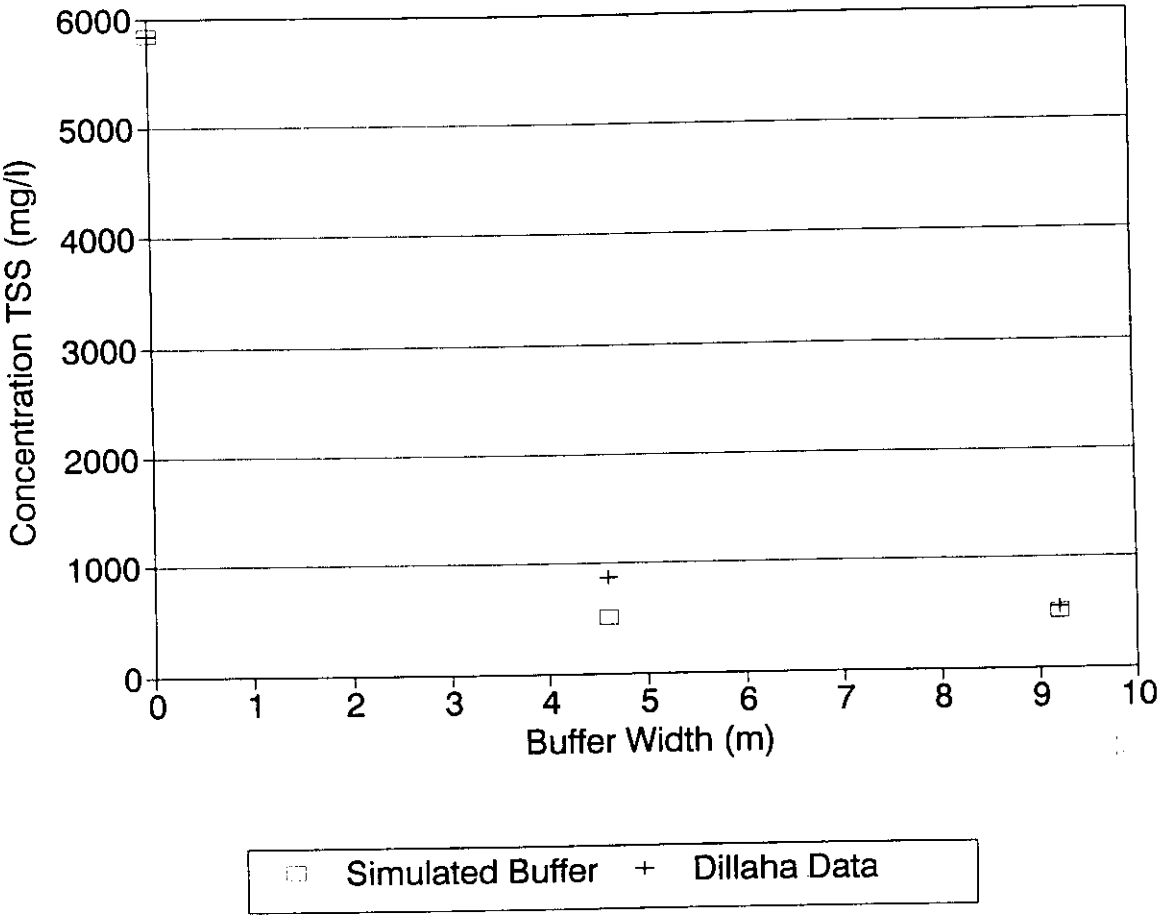

Figure 13: Total suspended solids concentration vs. buffer width. Simulated and field data from Dillaha et al. (1989) are shown.

Table 6: Results of model sensitivity analyses.

Variable	Value	TSS Predicted Results (mg/l)	Percent Change
Manning's n	0.075	1299.50	—
	0.110	713.53	-45.1
	0.150	396.56	-69.5
	0.180	267.32	-79.4
	0.045	3041.23	134.0
Soil Erodibility (K)	0.10	1299.50	—
	0.125	1299.50	0.0
	0.075	1299.50	0.0
Cover Factor (C)	0.004	1276.12	—
	0.002	1299.50	0.0
	0.006	1299.50	0.0

the data collected in the field study performed by Dillaha et al. (1989) was simulated. The results of the simulation of the Dillaha data are shown in Figure 13. The model predicted the TSS concentrations at the entrance and exit of the buffer very closely. The model over predicted the concentration of TSS at the 4.6 m buffer width by a factor of two.

4.4 Sensitivity Analyses

Sensitivity analyses were performed to determine the factors that influence the model the most. The only factors that are not set by the rainfall event or the geometric characteristics of the buffer itself are Manning's n, the USLE cover factor, C, and the USLE soil erodibility factor, K. The factors were increased and decreased by the same amount to determine the effects on the model output. The results were compared to a base set of factors simulating one of the storms from the field results on a mowed buffer. Results of sensitivity analyses performed on the model are in Table 6.

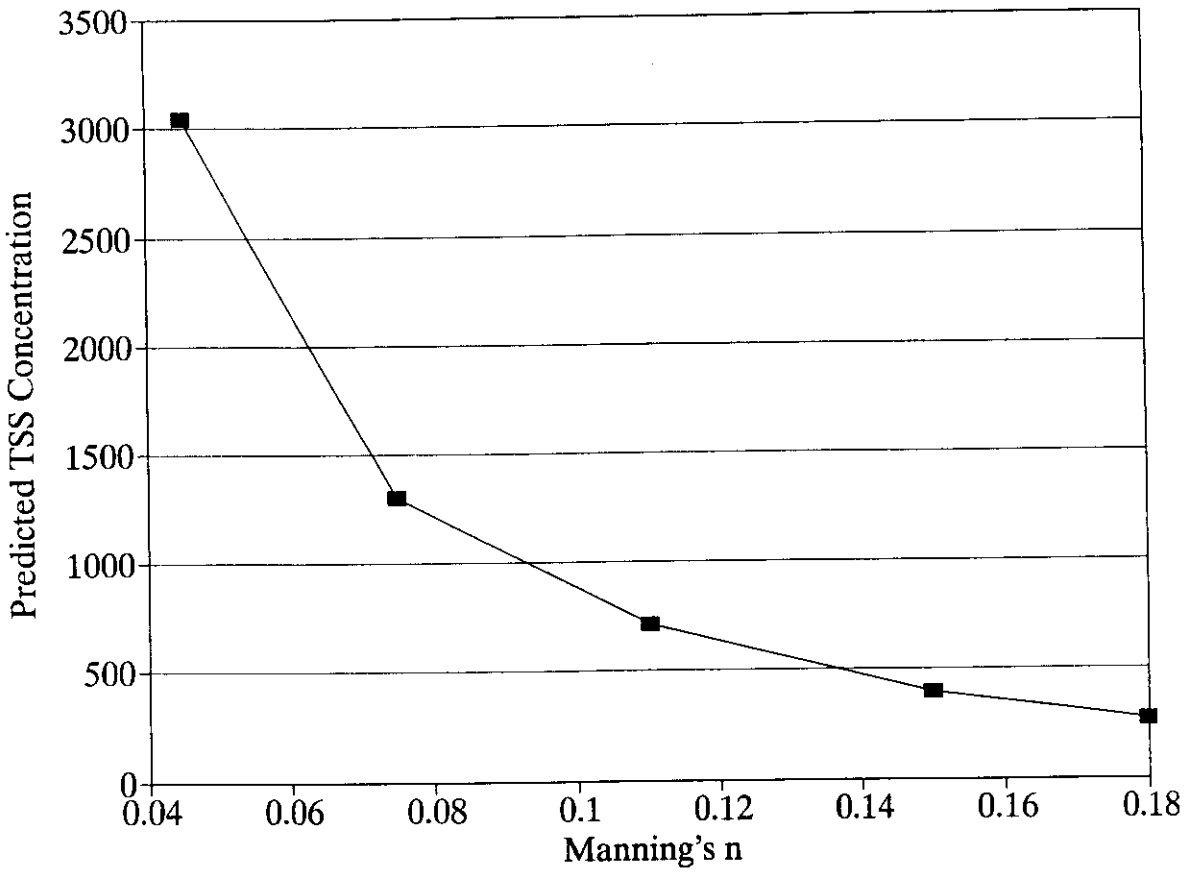

Figure 14: Relationship between Manning's n and predicted TSS concentrations.

Changing the value of Manning's n had a large effect on the final predicted concentration leaving the buffer. The value of 0.075 corresponded to a mowed buffer and was used as the base value. Increasing n to 0.150, the value used for unmowed buffers, decreased the predicted concentration of TSS by 69.5%. Decreasing the n value to 0.045 increased the predicted concentration of TSS by 134%. The predicted concentration decreased exponentially with increasing Manning's n (Figure 14).

Changing the USLE cover factor, C, or the soil erodibility factor, K, resulted in no change in the predicted concentration because transport capacity was the controlling factor in all cases tested. The cover factor and soil erodibility would affect the model results only in cases where detachment is the controlling factor at the end of the buffer. In such cases, the buffer would be too narrow to be of any use.

4.5 Discussion of Model Performance

The model predicted the long-term average concentrations of TSS in unmowed buffers for applications where the incoming concentration is below the transport capacity of the flow in the buffer strip. A direct comparison of predicted and actual long-term average concentration of TSS results in a coefficient of determination for all data points of 0.90 (Figure 15). Even though the model was able to predict long-term trends in concentrations it should not be used to predict mass loading for a single event in its present form.

It appears that the reduction of runoff due to transmission losses and, therefore, the reduction in transport capacity is one of the major contributors to buffer effectiveness in cases with low incoming concentrations.

One shortcoming of the model is that it predicts a maximum concentration rather than mass loading. The model may be modifed to compute mass loading but could not be tested or validated with existing field data. It may be that the maximum concentration increases but the mass loading decreases. By computing a maximum concentration and comparing to initial concentrations from field data the model tends to overpredict concentrations.

Changing the slope and/or buffer width to simulate other possible buffer designs helped to reinforce the conclusions of the field study. Changing the slope of the buffer from 10 to 5% decreased the predicted TSS concentration by 58%. Increasing the slope to 15% increased the predicted concentration by 66.3%. The relationships are directly proportional.

The results of varying the buffer width were mixed. Decreasing the buffer width from 12 m to 6 m resulted in a 5.5% decrease in the average predicted concentration. Increasing the buffer width to 18 m produced a decrease in predicted concentration of 1.2%. Upon further examination, it was revealed that for the shorter buffer, detachment was controlling the concentration in most cases because the transport capacity was not exceeded. For the longer buffer, transport capacity was the controlling factor. If the comparison is made with the transport capacity of the shorter buffer, decreasing the length results in an increase in

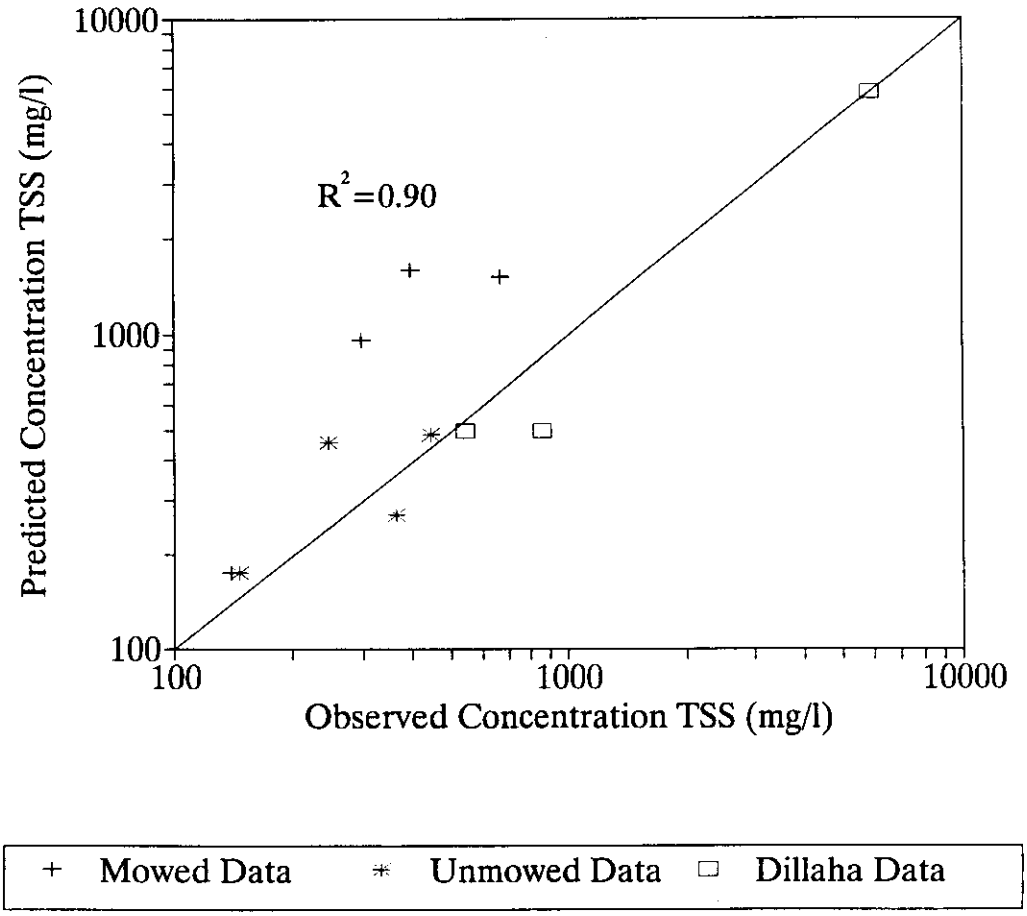

Figure 15: Predicted average concentrations of total suspended solids vs. actual average concentrations of total suspended solids.

predicted concentration.

Varying parameters used to compute infiltration rates, hydraulic conductivity and soil suction, had very small effects on the predicted sediment concentration. Changing hydraulic conductivity between 0.25 and 0.75 in/hr resulted in less than a 2% change in predicted concentration. Varying soil suction between 2.5 and 7.5cm resulted in changes of less than 1.5%.

The model was most sensitive to the value selected for Manning's n, therefore, the cover used in the buffer. The model was also sensitive to buffer length and slope to a lesser extent. These results show that increasing the slope or decreasing the length of the buffer decreases the effectiveness of the buffer. Changing cover type or density also affects buffer strip effectiveness as supported by the field study.

The results of the model concur with the conclusions of the field study and aid in the explanation of the processes in the buffer strip. The runoff entering the buffer strip was able to detach sediment and transport it within the buffer. The increase in TSS concentration resulted from an excess transport capacity of the runoff entering the buffer. As the runoff moved through the buffer, transport capacity became the dominant factor in determining TSS concentration. If steps are taken to reduce transport capacity at the end of the buffer like planting denser vegetation, lengthening the buffer or reducing the slope then the buffer will be more effective, although the concentrations of TSS and adsorbed pollutants leaving the buffer may be greater than the concentrations entering the buffer.

5 Conclusions

The first objective of the research was to determine the influences of vegetation composition, slope, buffer width, and infiltration rate on the effectiveness of native vegetation buffer zones as nonstructural treatment of urban runoff with respect to increasing water quality. To accomplish this, a field study was developed to collect runoff samples to create an urban buffer water quality dataset. Twelve pollutants were measured; fecal streptococci, fecal coliforms, dissolved nitrate, total nitrate, dissolved total phosphorus, total phosphorus, dissolved ammonia, total ammonia, dissolved total Kjeldahl nitrogen, total Kjeldahl nitrogen, total lead, and total suspended solids. Four different vegetation compositions were tested; wooded areas, wooded areas cleared, native grasses mowed, and native grasses unmowed.

Four hypotheses were tested to accomplish the first objective:

1. The vegetation composition of a buffer influences its effectiveness.
2. As the slope of a buffer strip increases, its effectiveness decreases.
3. As the width of a buffer strip increases, its effectiveness increases.
4. As the infiltration rate of the soil in a buffer increases, the buffer effectiveness increases.

For pollutants affected by vegetation composition, the wooded areas had higher mean concentrations of pollutants. The mowed and unmowed areas generally had the lowest concentrations of pollutants. Vegetation composition does significantly influence buffer effectiveness.

The effect of slope on buffer effectiveness was inconclusive. The slope of the buffers in this study changed within the buffer. It appears that as slope increases the buffer effectiveness decreases but further study is needed to confirm this.

For this application of buffer strips, it was found that as buffer width increased pollutant concentration also increased. Other researchers have reported decreasing pollutant concentrations. It is believed that the results in this study were caused by excess transport capacity

associated with the runoff entering the buffer strip. As the runoff moves through the buffer strip pollutants are detached and transported through the buffer strip. If the buffer strip is sufficiently wide, an equilibrium between transport capacity and detachment will be reached and a decrease in pollutant concentration may be seen due to reduced runoff.

Infiltration rate was highly correlated with vegetative cover as has been seen in other studies. The area with the highest infiltration rate, the wooded area, also had the highest mean pollutant concentration. Based on this, the hypothesis that as infiltration rate increases buffer effectiveness increases was rejected.

The second objective of the research was to determine the relative importance of vegetation composition, slope, buffer width, and infiltration rate on the effectiveness of native vegetation buffer zones. Results from the field study indicate that vegetative cover and buffer width are the two most important factors influencing buffer effectiveness.

The third study objective was to evaluate, and refine where possible, existing mathematical buffer strip models for applicability in urban areas. All existing models possess shortcomings making them unusable for urban buffers. A physically-based model was developed to simulate the buffer strips used in the field study. The model has a stochastic pollutant concentration input generator. Transport capacity is computed using the Yalin equation. Detachment and deposition are computed using the CREAMS method. The model was used to simulate this field study and the field study of other researchers. The model predicted the results of this field study with concentrations increasing with buffer width. The coefficient of determination for observed concentrations compared to predicted concentrations was 0.90.

The last objective of the research was to perform sensitivity analyses of the buffer strip model that best simulates urban buffer strips to determine the parameters influencing the model results and compare these to factors influencing buffer effectiveness determined by the field study. The model was most sensitive to the value selected for Manning's n which is related to vegetation composition. The buffer length also affected the model prediction. Transmission losses, affected by infiltration rates, were important to model performance.

Through the course of the research, several areas for further research were identified. Mass loading of pollutants were not computed in this study due to difficulties encountered in data collection by the City of Austin. It may be possible for the pollutant concentration to increase, but if a sufficient amount of runoff infiltrates then the mass loading may decrease. The amount of mass loading of pollutants is an area that requires further research. The concentration and mass loading of other urban pollutants such as organics, oil and grease, and heavy metals needs to be addressed.

The effects of dry deposition and deposition by rainfall need to be considered. Deposition of dust on the vegetation may increase sediment loads, and contaminants in the rainfall may increase other pollutant loads.

Several areas for further model development were also identified including simulation of other pollutants. The simulation of other pollutants may be helpful to urban planners in areas where these are of concern. The computation of mass loadings of pollutants is another area where the model may be modified.

References

1. Barfield, B.J., E.W. Tollner and J.C. Hayes. 1979. Filtration of sediment by simulated vegetation I. Steady-state flow with homogeneous sediment. *Transactions of the ASAE* 22(3):540–545,548.

2. Bingham, S.C., P.W. Westerman and M.R. Overcash. 1980. Effect of grass buffer zone length in reducing the pollution from land application areas. *Transactions of the ASAE* 23(2):330–335,342.

3. Blackburn, W.H., R.O. Meeuwig and C.M. Skau. 1974. A mobile infiltrometer for use on rangeland. *Journal of Range Management* 53:322-323.

4. Blake, R.G. and K.H. Hartge. 1986. Bulk density. p.363-376. In: A. Klute ed. *Methods of soil analysis. Part 1. Physical and mineralogical methods.* Agron. Ser. 9, ASA, SSSA, Madison WI.

5. Bufill, M.C. and M.J. Boyd. 1988. A flood study of three urban catchments near Sydney. Hydrology and Water Resources Symposium. Canberra, Australia.

6. Chow, V.T., D.R. Maidment and L.W. Mays. 1988. *Applied hydrology.* McGraw-Hill Book Co. New York.

7. Clinnick, P.F. 1985. Buffer strip management in forest: a review. *Australian Forestry* 48(1):34-45.

8. Dillaha, T.A. 1989. Water quality impacts of vegetative filter strips. ASAE Paper No. 89-2043. Am. Soc. Ag. Eng., St. Joseph, MI.

9. Dillaha, T.A., J.H. Sherrard, D. Lee, S. Mostaghimi and V.O. Shanholtz. 1985. Sediment and phosphorus transport in vegetative filter strips: Phase I, Field studies. ASAE Paper No. 85–2043. Am. Soc. Ag. Eng., St. Joseph, MI.

10. Dillaha, T.A., R.B. Reneau, S. Mostaghimi and D. Lee. 1989. Vegetative filter strips for agricultural nonpoint source pollution control. *Transactions of the ASAE* 32(2):513–519.

11. Doyle, R.C., G.D. Stranton and D.C. Wolf. 1977. Effectiveness of forest and grass buffer strips in improving water quality of manure polluted runoff. ASAE Paper No. 77–2501. Am. Soc. Ag. Eng., St. Joseph, MI.

12. Dunne, T., T.W. Cundy and W. Zhang. 1988. Effects of microtopography and vegetation cover density on infiltration and runoff. U.S. Geological Survey, PB89-178586.

13. Flanagan, D.C., G.R. Foster, W.H. Neibling and J.P. Burt. 1989. Simplified equations for filter strip design. *Transactions of the ASAE* 32(6):2001-2007.

14. Foster, G.R. and L.D. Meyer. 1972. Transport of soil particles by shallow flow. *Transactions of the ASAE* 15:99-102.

15. Foster, G.R., L.D. Meyer and C.A. Onstad. 1977. An erosion equation derived from basic erosion principles. *Transactions of the ASAE* 20:678-682.

16. Gee, G.W. and J.W. Bauder. 1986. Particle-size analysis. p.399-404. In: A. Klute ed. *Methods of soil analysis. Part 1. Physical and mineralogocal methods.* Agron. Ser. 9, ASA, SSSA, Madison WI.

17. Glick, R.H. 1992. *Native vegetation as nonstructural treatment of urban runoff.* M.S. Thesis in Agricultural Engineering. Texas A&M University, College Station, TX.

18. Green, W.H. and G.A. Ampt. 1911. Studies of soil physics part I.– the flow of air and water through soils. *Journal of Agriculture Science.* 4(1):1-24.

19. Hayes, J.C., B.J. Barfield and R.I. Barnhisel. 1979. Filtration of sediment by simulated vegetation II. Unsteady flow with non-homogeneous sediment. *Transactions of the ASAE* 22(5):1063–1067.

20. Huggins, L.F. and J.R. Burney. 1982. Surface runoff, storage and routing. p 169-225. In: Hann, C.T., H.P. Johnson and D.L. Brakensiek ed. *Hydrologic modeling of small watersheds.* ASAE Monograph No. 5. American Society of Agricultural Engineers. St. Joseph, MI. 533 pp.

21. Kao, D.K.T. and B.J. Barfield. 1978. Prediction of flow hydraulics for vegetated channels. *Transactions of the ASAE* 21(3):489-494.

22. Kelling, K.A. and A.E. Peterson. 1975. Urban lawn infiltration rates and fertilizer runoff losses under simulated rainfall. *Soil Sci. Soc. Am. Proc.* 39:348-352.

23. Kemper, W.D. and R.C. Rosenau. 1986. Aggregate stability and size distribution. p.425-442. In: A. Klute ed. *Methods of soil analysis. Part 1. Physical and mineralogical methods.* Agron. Ser. 9, ASA, SSSA, Madison WI.

24. Knisel, W.G., ed. 1980. *CREAMS: A field scale model for chemical, runoff, and erosion from agricultural management systems.* U.S. Department of Agriculture, Conservation Research Report No. 26. 640pp.

25. Law, A.M. and W.D. Kelton. 1982. *Simulation modeling and analysis.* McGraw-Hill, New York. 400 pp.

26. Lee, D. 1987. *Simulation of phosphorus transport in vegetative filter strips.* Ph.D. Dissertation, Virginia Polytechnic Institute and State University, Blacksburg VA. 207pp.

27. Lentner M. and T. Bishop. 1986. *Experimental design and analysis.* Valley Book Company. Blacksburg VA 24060. 565pp.

28. Lighthill, M.J. and G.B. Whitham. 1955. On kinematic waves 1. *Proc. Royal Soc.*, London, Ser. A, Vol 229:281-316.

29. Lowrance R., R. Todd, J. Fail, Jr., O. Hendrickson, Jr., R. Leonard, and L. Asmussen. 1984. Riparian forests as nutrient filters in agricultural watersheds. *BioScience* 34(6):374-377.

30. Marshall, T.J. and J.W. Holmes. 1979. *Soil physics.* Cambidge University Press. New York.

31. Mualem, Y. 1986. Hydraulic conductinity of unsaturated soils: prediction and formulas. In: A. Klute ed. *Methods of soil analysis. Part 1. Physical and mineralogical methods.* Agron. Ser. 9, ASA, SSSA, Madison WI.

32. Neibling, W.H. and E.E. Alberts. 1979. Composition and yield of soil particles transported through sod strips. ASAE Paper No. 79–2065. Am. Soc. Ag. Eng., St. Joseph, MI.

33. Nelson, D.W. and L.E. Sommers. 1986. Total carbon, organic carbon and organic matter. p.539-577. In: A. Page ed. *Methods of soil analysis. Part 2. Chemical and microbiological properties.* Agron. Ser. 9, ASA, SSSA, Madison WI.

34. Overcash, M.R., S.C. Bingham and P.W. Westerman. 1981. Predicting runoff pollutant reduction in buffer zones adjacent to land treatment sites. *Transactions of the ASAE* 24(2):430–435.

35. Parrish, J.H. and S. Stecher. 1991. Nonpoint pollution control in the City of Austin. Environmental and Conservation Services Department, Austin TX.

36. Phillips, J.D. 1989. An evaluation of the factors determining the effectiveness of water quality buffer zones. *Journal of Hydrology* 107(1):133-145.

37. Ree, W.O. 1949. Hydraulic characteristics of vegetated waterways. *Agricultural Engineering* 30(4):184–189.

38. Skaggs, R.W. 1982. Infiltration. In: Hann, C.T., H.P. Johnson and D.L. Brakensiek ed. *Hydrologic modeling of small watersheds.* ASAE Monograph No. 5. American Society of Agricultural Engineers. St. Joseph, MI. 533 pp.

39. Thurow, T.L., W.H. Blackburn, and C.A. Taylor, Jr. 1988. Infiltration and interrill response to selected livestock grazing strategies, Edwards Plateau, Texas. *Journal of Range Management* 41(4):296-301.

40. Tollner, E.W., B.J. Barfield, C.T. Haan and T.Y. Kao. 1976. Suspended sediment filtration capacity of simulated vegetation. *Transactions of the ASAE* 19(4):678–682.

41. Tollner, E.W., B.J. Barfield, C. Vachirakornwatana and C.T. Haan. 1977. Sediment deposition patterns in simulated grass filters. *Transactions of the ASAE* 20(5):940–944.

42. SAS Institute, Inc. 1988. *SAS/STAT user's guide, release 6.03.* SAS Institute Inc. Cary NC.

43. United States Department of Agriculture. 1974. *Soil survey of Travis County, Texas.* United States Department of Agriculture, Soil Conservation Service, Washington D.C.

44. United States Environmental Protection Agency. 1979. *Methods for chemical analysis of water and wastes.* EPA/600/4-79/020.

45. United States Environmental Protection Agency. 1990. *Risk assessment, management and communication of water contamination.* EPA/625/4-89/024. 147pp.

46. Whipple, W., N.S. Grigg, T. Grizzard, C.W. Randall, R.P. Shubinski, L.S. Tucker. 1983. *Stormwater management in urbanizing areas.* Prentice Hall. Englewood Cliffs NJ. 234 pp.

47. Wilson, L.G. 1967. Sediment removal from flood water by grass filtration. *Transactions of the ASAE* 10(1):35–37.

A Anova Tables

Table 7: Analysis of variance table for fecal streptococci.

General Linear Models Procedure

Dependent Variable: LOG

Source	DF	Sum of Squares	Mean Square	F Value	Pr > F
Model	7	34.65315050	4.95045007	1.33	0.2409
Error	117	434.50989365	3.71375977		
Corrected Total	124	469.16304415			

R-Square	C.V.	Root MSE	LOG Mean
0.073862	17.83184	1.927112	10.8071410

Source	DF	Type I SS	Mean Square	F Value	Pr > F
LOC	3	19.35769928	6.45256643	1.74	0.1631
COV	1	5.03150227	5.03150227	1.35	0.2468
LOC*COV	3	10.26394895	3.42131632	0.92	0.4329

Source	DF	Type III SS	Mean Square	F Value	Pr > F
LOC	3	18.41837531	6.13945844	1.65	0.1810
COV	1	9.95380270	9.95380270	2.68	0.1043
LOC*COV	3	10.26394895	3.42131632	0.92	0.4329

Table 8: Analysis of variance table for dissolve ammonia.

General Linear Models Procedure

Dependent Variable: LOG

Source	DF	Sum of Squares	Mean Square	F Value	Pr > F
Model	7	14.86820132	2.12402876	1.04	0.4034
Error	127	258.20389195	2.03310151		
Corrected Total	134	273.07209327			

R-Square	C.V.	Root MSE	LOG Mean
0.054448	-66.96864	1.425869	-2.1291587

Source	DF	Type I SS	Mean Square	F Value	Pr > F
LOC	3	1.31987475	0.43995825	0.22	0.8849
COV	1	3.23703297	3.23703297	1.59	0.2093
LOC*COV	3	10.31129360	3.43709787	1.69	0.1723

Source	DF	Type III SS	Mean Square	F Value	Pr > F
LOC	3	1.75402428	0.58467476	0.29	0.8343
COV	1	4.44943518	4.44943518	2.19	0.1415
LOC*COV	3	10.31129360	3.43709787	1.69	0.1723

Table 9: Analysis of variance table for dissolved nitrate.

General Linear Models Procedure

Dependent Variable: LOG

Source	DF	Sum of Squares	Mean Square	F Value	Pr > F
Model	7	14.57171262	2.08167323	3.40	0.0023
Error	130	79.58701676	0.61220782		
Corrected Total	137	94.15872938			

R-Square	C.V.	Root MSE	LOG Mean
0.154757	-174.3193	0.782437	-.44885272

Source	DF	Type I SS	Mean Square	F Value	Pr > F
LOC	3	2.69750380	0.89916793	1.47	0.2261
COV	1	10.88372884	10.88372884	17.78	0.0001
LOC*COV	3	0.99047998	0.33015999	0.54	0.6562

Source	DF	Type III SS	Mean Square	F Value	Pr > F
LOC	3	1.79678673	0.59892891	0.98	0.4052
COV	1	8.06408544	8.06408544	13.17	0.0004
LOC*COV	3	0.99047998	0.33015999	0.54	0.6562

Table 10: Analysis of variance table for dissolved total Kjeldahl nitrogen.

General Linear Models Procedure

Dependent Variable: LOG

Source	DF	Sum of Squares	Mean Square	F Value	Pr > F
Model	7	5.35856663	0.76550952	0.74	0.6408
Error	126	130.82971016	1.03833103		
Corrected Total	133	136.18827679			

R-Square	C.V.	Root MSE	LOG Mean
0.039347	825.2726	1.018985	0.12347257

Source	DF	Type I SS	Mean Square	F Value	Pr > F
LOC	3	1.24301857	0.41433952	0.40	0.7539
COV	1	2.33843001	2.33843001	2.25	0.1359
LOC*COV	3	1.77711805	0.59237268	0.57	0.6354

Source	DF	Type III SS	Mean Square	F Value	Pr > F
LOC	3	1.27871353	0.42623784	0.41	0.7457
COV	1	0.74281623	0.74281623	0.72	0.3993
LOC*COV	3	1.77711805	0.59237268	0.57	0.6354

Table 11: Analysis of variance table for dissolved total phosphorus.

General Linear Models Procedure

Dependent Variable: LOG

Source	DF	Sum of Squares	Mean Square	F Value	Pr > F
Model	7	23.12967574	3.30423939	3.61	0.0014
Error	131	119.99717713	0.91600899		
Corrected Total	138	143.12685287			

R-Square	C.V.	Root MSE	LOG Mean
0.161603	-79.23231	0.957084	-1.2079460

Source	DF	Type I SS	Mean Square	F Value	Pr > F
LOC	3	19.13763789	6.37921263	6.96	0.0002
COV	1	2.40742339	2.40742339	2.63	0.1074
LOC*COV	3	1.58461446	0.52820482	0.58	0.6314

Source	DF	Type III SS	Mean Square	F Value	Pr > F
LOC	3	20.96698795	6.98899598	7.63	0.0001
COV	1	0.47835590	0.47835590	0.52	0.4712
LOC*COV	3	1.58461446	0.52820482	0.58	0.6314

Table 12: Analysis of variance table for fecal coliforms.

Dependent Variable: LOG

Source	DF	Sum of Squares	Mean Square	F Value	Pr > F
Model	14	47.44099987	3.38864285	0.59	0.8731
Error	327	1879.38105995	5.74734269		
Corrected Total	341	1926.82205982			

R-Square	C.V.	Root MSE	LOG Mean
0.024621	32.22647	2.397362	7.43910670

Source	DF	Type I SS	Mean Square	F Value	Pr > F
LOC	3	7.91844926	2.63948309	0.46	0.7109
COV	3	0.13943238	0.04647746	0.01	0.9990
LOC*COV	8	39.38311824	4.92288978	0.86	0.5536

Source	DF	Type III SS	Mean Square	F Value	Pr > F
LOC	3	4.21497457	1.40499152	0.24	0.8653
COV	3	0.70996576	0.23665525	0.04	0.9888
LOC*COV	8	39.38311824	4.92288978	0.86	0.5536

Table 13: Analysis of variance table for total ammonia.

Dependent Variable: LOG

Source	DF	Sum of Squares	Mean Square	F Value	Pr > F
Model	14	17.06803586	1.21914542	0.45	0.9563
Error	423	1140.89729061	2.69715672		
Corrected Total	437	1157.96532646			

R-Square	C.V.	Root MSE	LOG Mean
0.014740	-76.85862	1.642302	-2.1367833

Source	DF	Type I SS	Mean Square	F Value	Pr > F
LOC	3	5.85364085	1.95121362	0.72	0.5384
COV	3	7.17548391	2.39182797	0.89	0.4479
LOC*COV	8	4.03891110	0.50486389	0.19	0.9926

Source	DF	Type III SS	Mean Square	F Value	Pr > F
LOC	3	5.28657660	1.76219220	0.65	0.5812
COV	3	6.58898805	2.19632935	0.81	0.4865
LOC*COV	8	4.03891110	0.50486389	0.19	0.9926

Table 14: Analysis of variance table for total nitrate.

Dependent Variable: LOG

Source	DF	Sum of Squares	Mean Square	F Value	Pr > F
Model	14	17.31517388	1.23679813	2.15	0.0091
Error	366	210.21218334	0.57435023		
Corrected Total	380	227.52735722			

R-Square	C.V.	Root MSE	LOG Mean
0.076102	-107.7715	0.757859	-.70320922

Source	DF	Type I SS	Mean Square	F Value	Pr > F
LOC	3	3.29834169	1.09944723	1.91	0.1268
COV	3	6.15773852	2.05257951	3.57	0.0142
LOC*COV	8	7.85909367	0.98238671	1.71	0.0945

Source	DF	Type III SS	Mean Square	F Value	Pr > F
LOC	3	1.63525708	0.54508569	0.95	0.4170
COV	3	7.38341379	2.46113793	4.29	0.0055
LOC*COV	8	7.85909367	0.98238671	1.71	0.0945

Table 15: Analysis of variance table for lead.

Dependent Variable: LOG

Source	DF	Sum of Squares	Mean Square	F Value	Pr > F
Model	14	53.32643495	3.80903107	6.55	0.0001
Error	409	237.76082055	0.58132230		
Corrected Total	423	291.08725550			

R-Square	C.V.	Root MSE	LOG Mean
0.183197	-19.13942	0.762445	-3.9836357

Source	DF	Type I SS	Mean Square	F Value	Pr > F
LOC	3	14.76171369	4.92057123	8.46	0.0001
COV	3	21.19937755	7.06645918	12.16	0.0001
LOC*COV	8	17.36534372	2.17066796	3.73	0.0003

Source	DF	Type III SS	Mean Square	F Value	Pr > F
LOC	3	20.46809232	6.82269744	11.74	0.0001
COV	3	23.16736122	7.72245374	13.28	0.0001
LOC*COV	8	17.36534372	2.17066796	3.73	0.0003

Table 16: Analysis of variance table for total suspended solids.

Dependent Variable: LOG

Source	DF	Sum of Squares	Mean Square	F Value	Pr > F
Model	14	100.8046147	7.2003296	5.26	0.0001
Error	428	585.3917502	1.3677377		
Corrected Total	442	686.1963649			

R-Square	C.V.	Root MSE	LOG Mean
0.146903	19.64818	1.169503	5.95222105

Source	DF	Type I SS	Mean Square	F Value	Pr > F
LOC	3	45.57945818	15.19315273	11.11	0.0001
COV	3	33.40412236	11.13470745	8.14	0.0001
LOC*COV	8	21.82103418	2.72762927	1.99	0.0457

Source	DF	Type III SS	Mean Square	F Value	Pr > F
LOC	3	42.61458213	14.20486071	10.39	0.0001
COV	3	40.76669431	13.58889810	9.94	0.0001
LOC*COV	8	21.82103418	2.72762927	1.99	0.0457

Table 17: Analysis of variance table for total Kjeldahl nitrogen.

Dependent Variable: LOG

Source	DF	Sum of Squares	Mean Square	F Value	Pr > F
Model	14	26.24706029	1.87479002	1.65	0.0637
Error	421	478.64111554	1.13691476		
Corrected Total	435	504.88817583			

R-Square	C.V.	Root MSE	LOG Mean
0.051986	102.1673	1.066262	1.04364286

Source	DF	Type I SS	Mean Square	F Value	Pr > F
LOC	3	10.96682922	3.65560974	3.22	0.0228
COV	3	7.55456524	2.51818841	2.21	0.0858
LOC*COV	8	7.72566583	0.96570823	0.85	0.5596

Source	DF	Type III SS	Mean Square	F Value	Pr > F
LOC	3	9.33694810	3.11231603	2.74	0.0431
COV	3	9.77961326	3.25987109	2.87	0.0363
LOC*COV	8	7.72566583	0.96570823	0.85	0.5596

Table 18: Analysis of variance table for total phosphorus.

Dependent Variable: LOG

Source	DF	Sum of Squares	Mean Square	F Value	Pr > F
Model	14	27.46985471	1.96213248	2.52	0.0018
Error	432	336.79828199	0.77962565		
Corrected Total	446	364.26813670			

R-Square	C.V.	Root MSE	LOG Mean
0.075411	-262.2651	0.882964	-.33666850

Source	DF	Type I SS	Mean Square	F Value	Pr > F
LOC	3	9.98531879	3.32843960	4.27	0.0055
COV	3	4.44499489	1.48166496	1.90	0.1288
LOC*COV	8	13.03954103	1.62994263	2.09	0.0355

Source	DF	Type III SS	Mean Square	F Value	Pr > F
LOC	3	8.10085266	2.70028422	3.46	0.0163
COV	3	7.25063820	2.41687940	3.10	0.0266
LOC*COV	8	13.03954103	1.62994263	2.09	0.0355

B Program Listing

```
C---ROGER GLICK, MARCH 1992, AGRICULTURAL ENGINEERING, TEXAS A&M.
C---THIS PROGRAM COMPUTES THE SEDIMENT CONCENTRATION AT SEVERAL
C---LOCATIONS IN A VEGETATIVE BUFFER. THE INPUT CONCENTRATION ENTERING
C---THE BUFFER IS REQUIRED AS WELL AS RAINFALL. RAINFALL LANDING IN THE
C---BUFFER IS ASSUMED TO INFILTRATE
C

      REAL UE, ZE, ERR,SC2(0:4),N,K
      INTEGER IX,I
      COMMON/BLK1/QT(0:4),DX,RT
      COMMON/BLK2/K, C, P, DET(3)
      COMMON/BLK3/DT, Q(0:6500,0:4), OT, RR(12)
      COMMON/BLK4/G, D(5), SG(5), SHX(37), SHY(37), PW, WS(3), TRA(3)
      COMMON/BLK5/CMEAN, SIG
      COMMON/BLK6/QMAX(0:4), YMAX(0:4), SP(3),N
      COMMON/BLK7/SC(0:4),INC(0:4)
      COMMON/BLK8/HC, SSM, FSM, PSI

        OPEN(UNIT=1,FILE='BUFFER.DAT',STATUS='UNKNOWN')
        OPEN(UNIT=2,FILE='TEST.OUT',STATUS='UNKNOWN')
      OPEN(UNIT=3,FILE='BUFFER.OUT',STATUS='UNKNOWN')

C---READING INPUT DATA FILE
      READ(1,*) IX
      CALL INPUT
C---COMPUTING OVERLAND FLOW PARAMETERS IN THE BUFFER.
      CALL OLFLOW
C---SIMULATING THE CONCENTRATION OF SEDIMENT ENTERING THE PARKING LOT
C---FROM THE DISTRIBUTION OF MEASURED DATA.
C---SETTING THE NUMBER OF REPETIONS FOR THIS STORM
      DO 101 NR=1,10
      WRITE(*,1) NR
  1   FORMAT(' ','NR = ',I3)
      UE=RAND(IX)
      CALL INVNOR(ZE,UE)
      ERR=ZE*SIG
      SC(0)=EXP(CMEAN+ERR)
      SC2(0)=SC(0)*(62.4/1000000)*QMAX(0)
C     WRITE(2,*) SC2(0), SC2(0)
C---COMPUTING THE MAXIMUM POSSIBLE SEDIMENT DETATCHMENT
      CALL DETAT
C---COMPUTING THE MAXIMUM TRANSPORT CAPACITY
      CALL TRANS
C---COMUTING THE SEDIMENT CONCENTRATION AND LOAD
      DO 10 I=1,3
       SC(I)=0
       DET(I)=(DET(I)+SC2(I-1))
```

```
48          IF(DET(I).GE.TRA(I)) GOTO 5
49          SC2(I)=DET(I)
50          INC(I)=1
51          GOTO 8
52      5   SC2(I)=TRA(I)
53          INC(I)=2
54      8   CONTINUE
55  C       WRITE(2,*) DET(I), TRA(I), INC(I)
56          IF(SC2(I).LE.0) GOTO 9
57           SC(I)=SC2(I)/(QMAX(i)*(62.4/1000000))
58          GOTO 10
59  c        SC(I)=((SC2(I)*(QT(I)/QMAX(I)))/(0T*60))
60  C       +                      /(QMAX(I)*(62.4/1000000))
61      9    SC(I)=0
62     10   CONTINUE
63  C---OUTPUTING DATA
64          CALL OUTPUT
65    101   CONTINUE
66          STOP
67          END
68
69  C
70  C        RANDOM NUMBER GENERATOR
71  C
72          FUNCTION RAND(IX)
73          INTEGER A,P,IX,B15,B16,XHI,XALO,LEFTLO,FHI,K
74          DATA A/16807/,B15/32768/,B16/65536/,P/2147483647/
75          XHI=IX/B16
76          XALO=(IX-XHI*B16)*A
77          LEFTLO=XALO/B16
78          FHI=XHI*A+LEFTLO
79          K=FHI/B15
80          IX=(((XALO-LEFTLO*B16)-P)+(FHI-K*B15)*B16)+K
81          IF(IX.LE.0) IX=IX+P
82          RAND=FLOAT(IX)*4.656612875E-10
83          RETURN
84          END
85  C
86  C        COMPUTE INVERSE OF NORMAL CDF
87  C
88          SUBROUTINE INVNOR(Z,CDF)
89          IF(CDF.LE.0.) CDF=1.E-10
90          IF(CDF.GE.1.) CDF=0.9999999
91          REL=CDF
92          IF(CDF.GT.0.5) REL=1.0-REL
93          T=SQRT(ALOG(1.0/REL/REL))
94          C1=2.515517+0.802853*T+0.010328*T*T
95          C2=1+1.432788*T+0.189269*T**2+0.001308*T**3
```

```
 96       Z=T-(C1/C2)
 97       IF(CDF.LT.0.5) Z=-Z
 98       RETURN
 99       END
100
101
102
103
104 C
105 C---THIS SUBROUTINE READS THE INPUT DATA FILE
106 C
107       SUBROUTINE INPUT
108       REAL N,K,XT
109       INTEGER J1,J2,J3,JJ,J,J4,OTH
110       COMMON/BLK1/QT(0:4),DX,RT
111       COMMON/BLK2/K, C, P, DET(3)
112       COMMON/BLK3/DT, Q(0:6500,0:4), OT, RR(12)
113       COMMON/BLK4/G, D(5), SG(5), SHX(37), SHY(37), PW, WS(3), TRA(3)
114       COMMON/BLK5/CMEAN, SIG
115       COMMON/BLK6/QMAX(0:4), YMAX(0:4), SP(3),N
116       COMMON/BLK8/HC, SSM, FSM, PSI
117 C
118 C---INPUTS FOR OVERLAND FLOW
119 C
120 C---READING SLOPE IN PERCENT
121       DO 3 J1=1,3
122        READ(1,*) SP(J1)
123        SP(J1)=SP(J1)/100
124    3  CONTINUE
125 C---SETTING MANNINGS FRICTION FACTOR, BASED ON COVER
126       READ(1,*) N
127 C---OVERLAND FLOW TIME INCREMENTS (SEC)
128       READ(1,*) DT
129 C---LENGTH OF SIMULATION (MIN)
130       READ(1,*) OT
131 C---SETTING SEGMENT LENGTHS (M)
132       READ(1,*) DX
133       DX=DX*3.281
134 C---INPUTING THE TOTAL RAINFALL DEPTH (IN)
135       READ(1,*) RT
136 C
137 C---INPUTS FOR RUNOFF FROM PARKING LOT
138 C
139       JJ=OT/(DT/60)
140       PRINT*, JJ
141       DO 5 J=0,JJ
142 C---PARKING LOT RUNOFF HYDROGRAPH (CFS)
143        READ(1,*) Q(J,0)
```

```
144    5  CONTINUE
145       PRINT*, Q(JJ,0)
146 C---MAXIMUM RUNOFF RATE (CFS)
147       READ(1,*) QMAX(0)
148 C---MAXIMUM DEPTH (IN)
149       READ(1,*) YMAX(0)
150 C---TOTAL RUNOFF (CU. FT.)
151       READ(1,*) QT(0)
152 C---NATURAL LOG OF THE MEAN CONCENTRATION (LN(MG/L))
153       READ(1,*) CMEAN
154 C---STANDARD DEVIATION OF THE MEAN CONCENTRATION
155       READ(1,*) SIG
156 C
157 C---INPUTS FOR DETATCHMENT
158 C
159 C---USLE SOIL ERODIBILITY FACTOR (K)
160       READ(1,*) K
161 C---USLE COVER MANAGEMENT FACTOR (C)
162       READ(1,*) C
163 C---USLE CONTOURING FACTOR (P)
164       READ(1,*) P
165 C
166 C---INPUTS FOR TRANSPORT COMPUTATION
167 C
168 C---ACCELERATION OF GRAVITY (FT/SEC**2)
169       READ(1,*) G
170 C---PARTICLE DISTRIBUTION DATA (D IN mm)
171       DO 10 J2=1,5
172        READ(1,*) D(J2), SG(J2)
173        D(J2)=(D(J2)/1000)*3.281
174    10 CONTINUE
175 C---READING IN COMPONENTS FOR THE SHIELDS DIAGRAM
176       DO 15 J3=1,37
177        READ(1,*) SHX(J3), SHY(J3)
178    15 CONTINUE
179 C---READING THE MASS DENSITY FOR THE TRANSPORTING FLUID
180       READ(1,*) PW
181 C---READING HOURLY RAINFALL RATES (IN/HR)
182       OTH=OT/60
183       DO 40 J4=1,OTH
184        READ(1,*) RR(J4)
185  40   CONTINUE
186 C---READING THE HYDRAULIC CONDUCTIVITY (IN/HR)
187       READ(1,*) HC
188 C---READING THE INITAL SOIL MOISTURE (IN)
189       READ(1,*) SSM
190 C---READING THE FINAL SOIL MOISTURE (IN)
191       READ(1,*) FSM
```

```
C--- AVERAGE SUCTION AT THE WETTING FRONT (IN)
      READ(1,*) PSI
      RETURN
      END

C
C---THIS SOLVES OVERLAND FLOW VOLUMES USING KIMEMATIC ROUTING
C
      SUBROUTINE OLFLOW
      REAL OT,N,S,SN(3),E,RE,QM,QL,YM,YP,bc,I(3),CI(3),R,HR
      INTEGER J,II,JJ,T,X, iot
      COMMON/BLK1/QT(0:4),DX,RT
      COMMON/BLK3/DT, Q(0:6500,0:4), OT, RR(12)
      COMMON/BLK6/QMAX(0:4), YMAX(0:4), SP(3),N

      DO 103 M3=1,3
      SN(M3)=(1.49/N)*(SP(M3)**.5)
      CI(M3)=0
 103  CONTINUE
        E=5./3.
C---SETTING INITIAL CONDITIONS T=0 AND X=0
      DO 8 II=1,3
       Q(0,II)=0
   8  CONTINUE
      Q(0,0)=0
C---TIME DO LOOP
      IOT=OT/(DT/60)
c     PRINT*, IOT
c     PRINT*, Q(IOT,0)
      td=dt/3600
      DO 20 T=1,IOT
C---SETTING RAINFALL RATES (IN/HR)
       HR=((((T*DT)/60)+60)/60)
       tt=t*dt/3600
c      print*, tt
       R=RR(INT(HR))
C---SETTING DISTANCE DO LOOP
       DO 10 X=1,3
                          QM=Q(T-1,X)
        QL=Q(T-1,X-1)
        YM=(QM/SN(X))**(0.6)
        yy=ym*12
        CALL INFIL(tT, Yy, I(x), CI(X), R, td)
c       print*, t, r
c       print*, x, ci(x)
c       Print*, t, x, yy
              RE=(R-I(x))/(12*3600)

```

```
240           YP=YM-(DT/DX)*(QM-QL)+RE*DT
241         IF (YP.LE.0) YP=0
242         Q(T,X)=SN(X)*(YP**E)
243         QT(X)=QT(X)+(.5*(Q(T,X)+Q(T-1,X))*DT)
244         IF (Q(T,X).le.QMAX(X)) goto 10
245         QMAX(X)=Q(T,X)
246         YMAX(X)=(QMAX(X)/SN(X))**(0.6)
247    10  CONTINUE
248    20 CONTINUE
249 C---DATA OUTPUT
250         DO 90 J=0,IOT
251       BC=J/6.
252          WRITE(2,65) BC, Q(J,0),Q(J,1),Q(J,2),Q(J,3)
253   65     FORMAT(' ',10X,f8.3,7X,F10.7,7X,F10.7,7X,F10.7,7X,F10.7)
254   90  CONTINUE
255       RETURN
256         END
257
258
259
260
261
262
263
264 C
265 C---THIS SUBROUTINE COMPUTES SEDIMENT DETATCHMENT USING THE CREAMS
266 C---EQUATIONS.
267 C
268       SUBROUTINE DETAT
269       REAL EI, R, S, SA, K,DI(3),DR(3),N
270       INTEGER NS
271       COMMON/BLK1/QT(0:4),DX,RT
272       COMMON/BLK2/K, C, P, DET(3)
273       COMMON/BLK6/QMAX(0:4), YMAX(0:4), SP(3),N
274
275 C
276 C---COMPUTING EI, FROM P.44 OF CREAMS MANUAL
277 C
278       EI=8.0*(RT**1.51)
279       DO 10 NS=1,3
280 C
281 C---COMPUTING EROSION CONSTANTS
282 C
283       R=K*C*P*(QMAX(NS)/QT(NS))
284       IF(QT(NS).LE.0) R=0
285 C
286 C---COMPUTING SINE OF THE SEGMENT SLOPE
287 C
```

```
288       SA=ATAN(SP(NS))
289       S=SIN(SA)
290 C
291 C---COMPUTING INTERRILL EROSION
292 C
293       DI(NS)=0.21*EI*(S+0.014)*R
294 C
295 C---COMPUTING RILL EROSION
296 C
297       DR(NS)=37983.*2.*QT(NS)*(QMAX(NS)**(1./3.))
298      +         *((DX/72.6)**(2.-1.))*(S**2.)*R
299       DET(NS)=(DI(NS)+DR(NS))*DX
300    10 CONTINUE
301       RETURN
302       END
303
304 C
305 C---THIS SUBROUTINE COMPUTES TRANSPORT CAPACITY USING YALIN'S EQN. AS
306 C---MODIFIED BY FOSTER AND MEYERS (1972).
307 C
308       SUBROUTINE TRANS
309       REAL TAU(3), YCRIT(5), A(5), Y(5), DEL(5), N,S(3),Y1(3),
310      +       T, SIG(5),P(5), PE(5), W(5), VS(3), REYN(5)
311       INTEGER K, J, NS, I
312       COMMON/BLK4/G, D(5), SG(5), SHX(37), SHY(37), PW, WS(3), TRA(3)
313       COMMON/BLK6/QMAX(0:4), YMAX(0:4), SP(3),N
314
315
316       DO 100 NS=1,3
317       WS(NS)=0
318       T=0
319       SA=ATAN(SP(NS))
320       S(NS)=SIN(SA)
321       Y1(NS)=(QMAX(NS)*(0.01/(S(NS)**0.5)))**0.6
322       TAU(NS)=PW*32.2*Y1(NS)*S(NS)*((0.01/N)**0.9)
323       VS(NS)=(TAU(NS)/PW)**0.5
324 C---COMPUTING YCRIT, DEL, AND T
325       DO 30 K=1,5
326        REYN(k)=(VS(NS)*D(K))/1.05E-5
327       J=0
328       DO 5 J=1,37
329        IF (REYN(K).LE.0.25) YCRIT(K)=0.45
330        IF (REYN(K).LE.0.25) GOTO 5
331        IF (REYN(K).GE.SHX(J)) GOTO 5
332        YCRIT(K)=SHY(J)-(((SHY(J)-SHY(J-1))/SHX(J)-SHX(J-1))*
333      +                 (SHX(J)-REYN(k)))
334        GOTO 6
335    5  CONTINUE
```

```
336     6   A(K)=2.45*(SG(K)**(-0.4))*(YCRIT(K)**(0.5))
337         Y(K)=VS(NS)**2/((SG(K)-1.0)*G*D(K))
338         IF (Y(K).LT.YCRIT(K)) GOTO 10
339         DEL(K)=(Y(K)/YCRIT(K))-1
340         GOTO 20
341    10   DEL(K)=0
342    20   SIG(K)=A(K)*DEL(K)
343         T=T+DEL(K)
344         IF(DEL(K).EQ.0) GOTO 25
345         P(K)=0.635*DEL(K)*(1-(1/SIG(K))*LOG(1+SIG(K)))
346         GOTO 30
347    25   P(K)=0
348    30    CONTINUE
349        DO 40 I=1,5
350         IF(T.LE.0) PE(I)=0
351         IF(T.LE.0) GOTO 31
352         PE(I)=(P(I)*DEL(I))/T
353    31   W(I)=PE(I)*SG(I)*PW*G*D(I)*VS(NS)
354         WS(NS)=WS(NS)+W(I)
355    40 CONTINUE
356         TRA(NS)=WS(NS)
357   100 CONTINUE
358        RETURN
359        END
360
361 C
362 C---THIS SUBROUTINE WRITES THE SIMULATED DATA TO A FILE
363 C
364        SUBROUTINE OUTPUT
365        COMMON/BLK7/SC(0:4), INC(0:4)
366
367        DO 10 J=0,3
368         WRITE(3,5) J, SC(J), INC(J)
369    10   CONTINUE
370     5   FORMAT(' ',5X,I2,5X,F10.2,5X,I2)
371        RETURN
372        END
373
374
375
376 C
377        subroutine INFIL(t, h, i, F, R, td)
378        COMMON/BLK8/HC, SSM, FSM, PSI
379
380 C
381 C  This subroutine computes the infiltration using the Green & Ampt equatio
382 C
383 C
```

```
C --VARIABLES--
C
C       INPUT:  HC = hydraulic conductivity (in/hr)
C               SSM = initial soil moisture at t=0 (in)
C               FSM = final soil moisture =  effective porosity (in)
C               PSI = average soil suction at the wetting front (in)
C               R = rainfall rate (in/hr)
C               ho = depth of ponding on soil surface (in)
C               time = time in hrs
C  CALCULATED:  i = infiltration rate (in/hr)
C               F = cumulative infiltration since t=0 (in)
C
      real DIFF, h, t, F0, F1, i, F, R, ism, i0
C
C  Initial settings
C
      DIFF = 1.0
      F0 = F
C
C     Check to see if ponding height is greater than soil suction head
C
c      IF (h .GE. PSI) GOTO 120
C
C     Solve for Cumulative Infiltration iteratively
C
c 100  F1 = HC*t + (PSI+h)*(FSM-SSM)*LOG(1 + (F0/((PSI+h)*(FSM-SSM) )))
  100  f1=f0+i*td
       i0 = HC * (PSI + h) * (FSM-SSM)/F1 + HC
       IF ((i0*td) .GT. ((R*td) + h)) then i0=(r*td)+h
       DIFF = ABS(i-i0)
       i=i0
       IF (DIFF .GE. 0.0001) GOTO 100
C
C     Determine Infiltration Rate
C
       f=f0+i*td

       RETURN
C
  120  WRITE (*,130)
  130  FORMAT ('0', 'WARNING:  Ponding height > soil suction potential')
       RETURN
       END
```